FATIGUE STRENGTH ANALYSIS OF A TYPICAL HIGHWAY SIGN FACE TO POST CONNECTION

by

Surapong Tovichakchaikul

Submitted in Partial Fulfillment of the Requirements
for the Degree of
Master of Science in Engineering
in the
Mechanical Engineering
Program

Frank J Tarantine Dec. 21, 1977
Advisor Date

Dean of Graduate School January 3, 1978
Date

YOUNGSTOWN STATE UNIVERSITY

March, 1978

ABSTRACT

FATIGUE STRENGTH ANALYSIS OF A TYPICAL HIGHWAY SIGN FACE TO POST CONNECTION

Surapong Tovichakchaikul

Master of Science in Engineering

Youngstown State University, Year 1978.

The objective of this thesis can be divided into two basic parts. The first part was to analyze and formulate equations involving stress and deflection of the sign face-to-post connection, in order to better understand the effects when fatigue loads are applied. The equations for deflection were formulated based on simple beam theory and plate theory. Experiments were performed using strain-gages to verify the analytical method and results obtained. Typical examples were conducted and are included to compare the theoretical and experimental results.

The second part was to investigate the fatigue properties of current and proposed sign face connection systems by subjecting them to mechanical oscillatory-type bending tests on a fatigue testing machine.

ACKNOWLEDGEMENTS

The author wishes to express his sincere gratitude and appreciation to his advisor, Dr. Frank J. Tarantine, whose generous help, encouragement and guidance throughout this thesis was invaluable.

I am deeply grateful to my dearly beloved parents, Mr. and Mrs. Tovichakchaikul, for their encouragement and inspiration for higher education.

TABLE OF CONTENTS

	PAGE
ABSTRACT	ii
ACKNOWLEDGEMENTS	iii
TABLE OF CONTENTS	iv
LIST OF SYMBOLS	vi
LIST OF FIGURES	viii
LIST OF TABLES	x
CHAPTER	
I. INTRODUCTION	1
II. THEORETICAL ANALYSIS	6
2.1 Introduction	6
2.2 Mathematical Analysis	6
III. THE MEASUREMENT OF EXPERIMENTAL STRESSES IN THE BOLT AND SIGN FACE	30
3.1 Introduction	30
3.2 Stress Distribution in the Sign Face after the Bolt Has Been Tightened	32
3.3 Strain Readings in the Bolt after Application of Tensile Load(s)	37
3.4 Strain Readings in the Bolt after Tightening the Bolt Nut	39
3.5 The Relationship between the Bolt Tension and Tightening Torques	40
3.6 Stress Distribution in the Sign Face when an External Load Applied	46
3.7 Bolt Strain Readings with an External Load Applied to the Post-Face Connection	59
IV. EXPERIMENTAL FATIGUE INVESTIGATION	72

PAGE

4.1 Introduction 72

4.2 Standard Connection 73

4.2.1 Testing Procedures and Results . . 74

4.3 Modified Connection 81

4.3.1 Testing Procedures and Results . . 81

4.4 Connection with a Proposed Back-Up Plate 86

4.4.1 Testing Procedures and Results . . 86

V. CONCLUSIONS AND DISCUSSION 94

5.1 Conclusions 94

5.2 Discussion 96

APPENDIX A 102

REFERENCES 105

LIST OF SYMBOLS

SYMBOL	DEFINITION	UNITS OR REFERENCE
A_b	Cross-sectional area of bolt	$in.^2$
b	Width of the central segment of sign face	in.
D	Diameter of bolt	in.
E	Young's modulus of elasticity	psi
E_b	Young's modulus of elasticity of bolt material	psi
E_{sf}	Young's modulus of elasticity of sign face material	psi
F_e	External load	See Figure 7
F_i	Initial tensile preload	See Figure 4
F_i^a	Tensile force in the bolt	See Figure 8
F_i^b	Tensile force in the bolt	See Figure 12
F_R	Reaction force	See Figure 4
I	Moment of inertia of the sign face cross-sectional area	$in.^4$
I_A	Moment of inertia at point A	See Eq. (2-46)
I_E	Moment of inertia at point E	See Eq. (2-40)
ℓ	Span of sign face	in.
ℓ_b	Length of the bolt	in.
M	Bending moment	lb-in.
M_A	Bending moment at point A	lb-in.
M_E	Bending moment at point E	lb-in.
r	Radius of mounting holes of the sign face	in.
R^a	Reaction force	See Figure 8
R^b	Reaction force	See Figure 12
T	Initial bolt tightening torque	lb-in.

SYMBOL	DEFINITION	UNITS OR REFERENCE
t	Thickness of sign face	in.
x	Distance between the edges of the post	in.
δ_b	Deformation of the bolt	See Eq. (2-6)
δ_B	Deflection at point B	See Figure 11
δ_E	Deflection at point E	See Figure 11
δ_f	Maximum deflection at mid-span	See Figure 10a
δ_{Fe}	Deflection at mid-span	See Figure 11
δ_{Fi}	Deflection at mid-span	See Eq. (2-9)
$\delta_R{}^a$	Deflection at mid-span	See Figure 10c
$\delta_R{}^b$	Deflection at mid-span	See Figure 14
$\Delta\delta_b$	Change of deformation in bolt stretch	See Eq. (2-15)
ΔF_i	Change of tensile force	See Eq. (2-12)
σ	Bending stress	See Eq. (2-36)
$\sigma_{avg.}$	Average bending stress	psi
σ_A	Bending stress at point A	psi
σ_b	Tensile stress in bolt	psi
σ_E	Bending stress at point E	psi
ϵ	Strain	none
ν_{Al}	Poisson's ratio of Aluminum	none

LIST OF FIGURES

FIGURE		PAGE
1.	Assembly Drawing of the Designed Loading Frame	3
2.	Photograph of MTS Direct Loading Arrangement	3
3.	Schematic of Fastening Bolt	6
4.	Free Body Diagram of a Post Section when the Bolt Has Been Tightened	8
5.	Free Body Diagram of Sign Face Section when the Bolt Has Been Tightened	9
6.	Loading, Shear and Moment Diagrams	10
7.	The External Load, F_e, Applied	11
8.	Free Body Diagram of Post with Load F_e Applied, Case (a)	12
9.	Free Body Diagram of the Sign Face with External Load F_e Applied, Case (a)	13
10.	Deflection by Superposition	14
11.	Loading, Shear and Moment Diagrams	15
12.	Free Body Diagram of Post with External Compressive Load F_e Applied, Case (b)	17
13.	Free Body Diagram of the Sign Face with the External Load F_e Applied, Case (b)	19
14.	Deflection by Superposition	19
15.	Concentrated Load Applied at the Center of the Mounting Hole Area	26
16(a)	Concentrated Load at the Mid-Point of the Plate	26
16(b)	Concentrated Load at the Mid-Point of the Beam	26
17.	The Gages were bonded to the Sign Face	32
18.	Strain Readout Instruments	33
19.	Distribution of Stresses along the x Axis	36

FIGURE		PAGE
20.	Photograph of the Tensile Load Applied to the Bolt	38
21.	Photograph of a Calibrated Torque Wrench and Strain Readout Instruments	39
22.	Bolt Strain Readings as a Function of Tension	41
23.	Bolt Strain Readings as a Function of Tightening Torque	42
24.	Distribution of Stresses along the x Axis, when an External Tensile Load Has Been Applied	51
25.	Distribution of Stresses along the x Axis, when an External Compressive Load Has Been Applied	52
26.	Photograph of Standard Connection	73
27.	Photograph of Typical Cracks for Standard Connection	80
28.	Photograph of Modified Connection	85
29.	Photograph of Half Pipes	85
30.	Photograph of Typical Cracks for Modified Connection	86
31.	Photograph of Connection with a Proposed Back-Up Plate	90
32.	Photograph of Back-Up Strip	90
33.	Photograph of Typical Cracks by Using Proposed Back-Up Plate	92
34.	Fluctuating Stress in the Sign Face at the Mounting Hole Area	98
35.	Fluctuating Stress in the Bolt	99

LIST OF TABLES

TABLE		PAGE
1.	Surface Strains in the Sign Face VS Bolt Tightening Torque	34
2.	Surface Stresses in the Sign Face VS Bolt Tightening Torque	35
3.	Strain Readings in the Bolt VS Applied Tensile Loads	38
4.	Strain Readings in the Bolt VS Bolt Tightening Torque	40
5.	Tensile Load on Bolt VS Bolt Tightening Torque	44
6.	Coefficient of Thread Friction	45
7.	Surface Strains in the Sign Face when an External Tensile Load Has Been Applied	47
8.	Surface Strains in the Sign Face when an External Compressive Load Has Been Applied	48
9.	Surface Stresses in the Sign Face when an External Tensile Load Has Been Applied	49
10.	Surface Stresses in the Sign Face when an External Compressive Load Has Been Applied	50
11.	Bolt Strain Readings at Hole C, with a Tensile-Type External Load Applied	61
12.	Bolt Strain Readings at Hole C, with a Compressive External Load Applied	62
13.	Bolt Strain Readings at Holes A, B, and C with a Tensile-Type External Load Applied	63
14.	Bolt Strain Readings at Holes A, B and C with a Compressive External Load Applied	64
15.	Tabulation of Fatigue Tests Using a Standard Connection	75
16.	Tabulation of Fatigue Tests Using a Modified Connection	82
17.	Tabulation of Fatigue Tests Using a Proposed Back-Up Plate	87

CHAPTER I

INTRODUCTION

The fatigue strength of a typical highway sign face-to-post connection is affected by many factors. From fatigue investigations conducted in the past [1],[1] it was found, for example, that the fatigue strength of a sign can be improved with the use of flat washers between the bolt head and sign blank. In some cases, the use of local back-up devices supporting the under-side of the sign blank were also found to improve the fatigue life. However, it was found that one of most damaging elements that leads to an early fatigue failure of a sign face is the "over-torqueing" of the fastener bolts. Since there are not much data available in the open literature on this subject, this investigation is directed toward the development of an improved sign blank fatigue life by means of experimental fatigue studies and mathematical analyses.

It is known that a fatigue failure of a highway sign is caused by the dynamic loading resulting from the oscillatory motion effect of the wind. It has further been found that the

---

[1]Numbers in brackets designate references listed on page 105.

most critically stressed sections of the sign face are in the mounting hole area and along the edge of the post, or line of contact between post and face. Consequently, the purpose of this study was:

1. to investigate the factors affecting the fatigue strength of the face for a standard connection;
2. to determine the fatigue strength of the face with a modified post-to-face connection; and,
3. to determine the fatigue strength of the face when using a proposed back-up device.

By the nature of their design, it was reasonable to expect that the modified post-to-face connection and the use of the proposed back-up device would improve the fatigue strength of the face along the edge of the post as well as in the fastener area.

From a previous investigation on highway signs [1], it was found that the state of stress induced by wind loading on a sign face is primarily one of bending caused by both wind pressure acting directly on the face and by the dynamic loading effect resulting from the inertia and vibratory motion of the sign. As a result, it was felt that a representative fatigue test of the sign blank can be obtained by directly loading the sign blank material, connected to a standard post, with an oscillating-type bending load.

In order to obtain this type of load, it was necessary to design a loading frame for this purpose. Figure 1 shows the assembly drawing of the loading frame as finally designed.

Figure 2 shows the loading arrangement using the loading frame in the Mechanical Engineering Department's Material Testing System (MTS), fatigue testing machine.

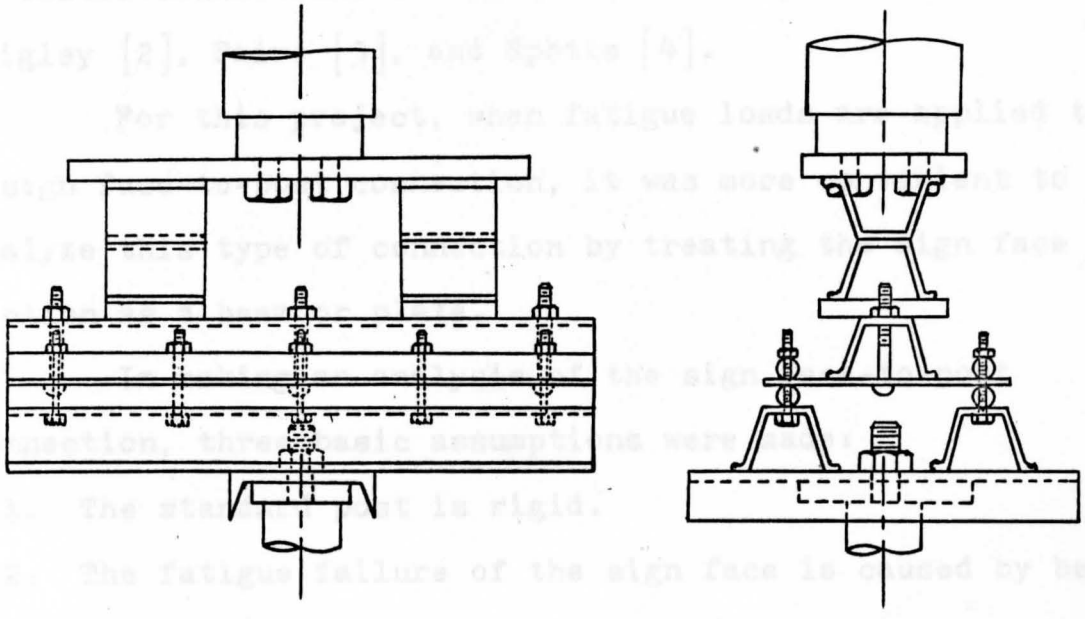

Figure 1 Assembly Drawing of the Designed Loading Frame

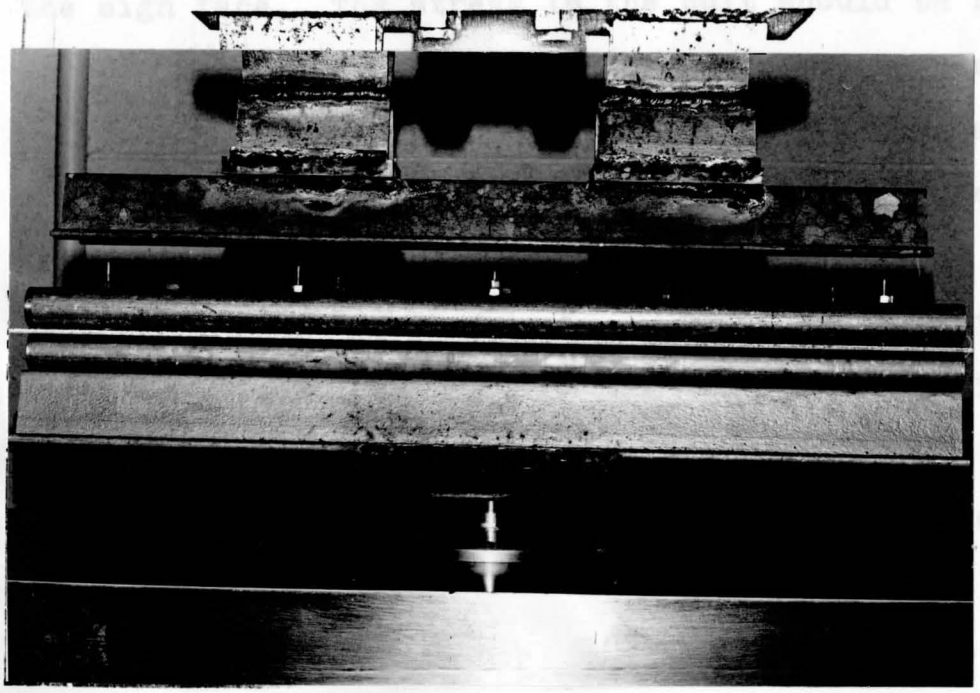

Figure 2 Photograph of MTS Direct Loading Arrangement

The mathematical analysis of bolted connections under cyclic loading are commonly encountered in various analytical design problems. Notable work related to the design aspects of bolted connections can be found in the publications of Shigley [2], Faire [3], and Spotts [4].

For this project, when fatigue loads are applied to a sign face-to-post connection, it was more convenient to analyze this type of connection by treating the sign face section as a beam or plate.

In making an analysis of the sign face-to-post connection, three basic assumptions were made:

1. The standard post is rigid.
2. The fatigue failure of the sign face is caused by bending stresses only.
3. The fatigue strength of the bolt is larger than that for the sign face. The stress in the bolt should be kept below the elastic limit at all times. If the stress in the bolt exceeds the elastic limit, plastic elongation of the bolt will occur, resulting in a loosening of the bolted connection [5].

Also, in conducting this analysis, the stress at any point in the face is determined by assuming static loading. Based on the above assumptions, the fatigue strength at any point of interest and the fatigue strength of the bolt can be obtained.

A secondary purpose of this study was to obtain a comparison between the stresses from experimental and

formulated equations at a given point in the sign blank, and, in the bolt under the same loading conditions.

CHAPTER II

THEORETICAL ANALYSIS

2.1 Introduction

In order to analyze the typical Highway sign face to post connection, when fatigue loads were applied, it was necessary to determine:

1. the tensile force and stress in the bolt,
2. the bending stress in the sign face along the line of contact between the edge of the post and face, and,
3. the stress at the mounting hole

for three different loading conditions.

2.2 Mathematical Analysis

The fastener bolts are tightened by applying torque to the bolt's nut as shown schematically in Figure 3.

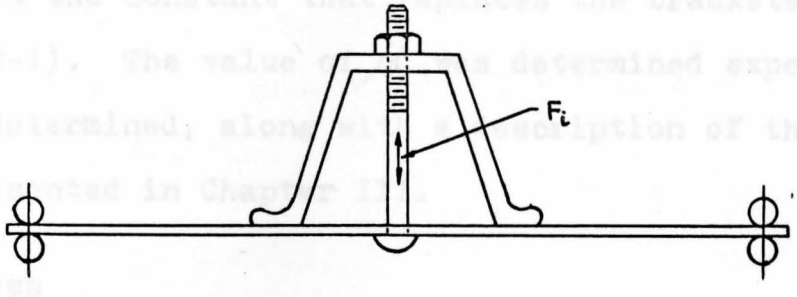

Figure 3 Schematic of Fastening Bolt

Bolt Force

If the forces in a screw are analyzed by considering the developed helix to be an inclined plane, the following equation relating tensile force to torque is obtained [4]:

$$T = DF_i\left[\frac{\cos\theta\tan\alpha+\mu_1}{2\cos\theta-\mu_1\tan\alpha} + \frac{1}{2}\left(\frac{r_c}{r_t}\right)\mu_2\right] . \quad (2\text{-}1)$$

The bracketed term in equation (2-1) involves: (1) coefficient of friction terms μ_1 and μ_2 which represent the coefficient of thread friction and the coefficient of friction for the collar respectively; (2) the angles α and θ which are the helix angle and the thread angle respectively; and, (3) the radii r_c and r_t which are the collar radius and the pitch radius of the thread respectively. Since all of the above terms are constant for a particular size and type of bolt used with a given application, equation (2-1) may be written as

$$T = \mu D F_i , \quad (2\text{-}2)$$

where μ is the constant that replaces the bracketed term of equation (2-1). The value of μ was determined experimentally. The value determined, along with a description of the experimental work is presented in Chapter III.

Normal Stress

The average tensile stress normal to the bolt's cross section for an initial tensile preload F_i is given by:

$$\sigma_i = \frac{F_i}{A_b} = \frac{4F_i}{\pi D^2} \quad . \quad (2\text{-}3)$$

Free Body Diagram

When an initial torque or tensile preload, F_i , has been applied, the bolt will undergo a deformation due to this load.

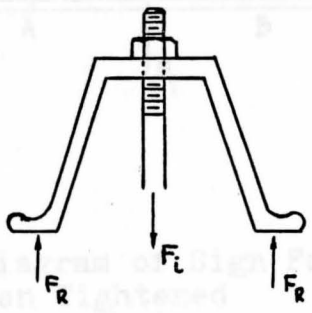

Figure 4 Free Body Diagram of a Post Section when the Bolt has been tightened

From Figure 4, considering static equilibrium in the vertical direction:

$$F_R = \frac{F_i}{2} \quad . \quad (2\text{-}4)$$

Substituting F_i from equation (2-2) into equation (2-4) gives:

$$F_R = \frac{T}{2\mu D} \quad . \quad (2\text{-}5)$$

Using Hooke's Law, the deformation caused by the preload, F_i , in the bolt is given by:

$$\delta_b = \frac{F_i l_b}{A_b E_b} \quad ,$$

or,

$$\delta_b = \frac{F_i}{K_b} \quad , \quad (2\text{-}6)$$

where,

$$K_b = \frac{A_b E_b}{l_b} \quad . \quad (2\text{-}7)$$

Substituting equations (2-4) and (2-5) into (2-6) gives:

$$\delta_b = \frac{T}{\mu D K_b} \qquad (2\text{-}8)$$

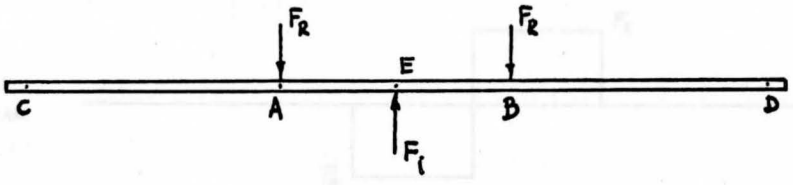

Figure 5 Free Body Diagram of Sign Face Section when the bolt Has Been Tightened

Using the equilibrium equation and neglecting the weight of the sign face in Figure 5, the reaction forces at the fixed supports C and D are equal to zero.

Therefore, the deformation of the sign face will only occur between points A and B.

Moment Area Method Applied to Sign Face:

It was necessary to draw a moment diagram for considering the bending occuring with the sign face. Accordingly, drawn in Figure 6 are the loading, shear and moment diagrams for a section of sign face subjected to initial bolt load.

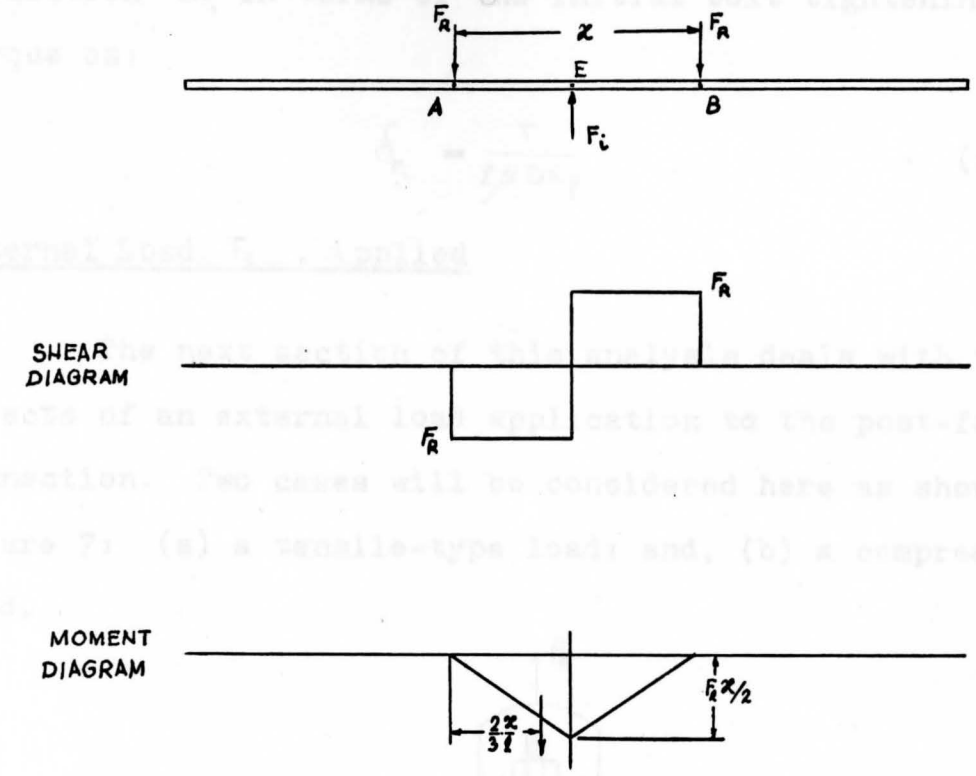

Figure 6 Loading, Shear and Moment Diagram

From Figure 6, the maximum deflection of the sign face due to the bolt load can be determined by using simple bending theory and the moment area method as follows:

$$E_{sf} I \, \delta_{F_i} = \frac{1}{2} \cdot \frac{F_R x}{2} \cdot \frac{x}{2} \cdot \frac{2}{3} \cdot \frac{x}{2} \quad ,$$

$$E_{sf} I \, \delta_{F_i} = \frac{F_R x^3}{24} \quad .$$

Dividing by $E_{sf}I$ gives:

$$\delta_{F_i} = \frac{F_R x^3}{24 E_{sf} I} = \frac{F_R}{K_p} \quad , \qquad (2\text{-}9)$$

where,

$$K_p = \frac{24 E_{sf} I}{x^3} \quad . \qquad (2\text{-}10)$$

Substituting Equation (2-5) into (2-9), gives the face deflection δ_{F_i} in terms of the initial bolt tightening torque as:

$$\delta_{F_i} = \frac{T}{2\mu D K_p} \qquad (2\text{-}11)$$

External Load, F_e, Applied

The next section of this analysis deals with the effects of an external load application to the post-face connection. Two cases will be considered here as shown in figure 7; (a) a tensile-type load; and, (b) a compressive load.

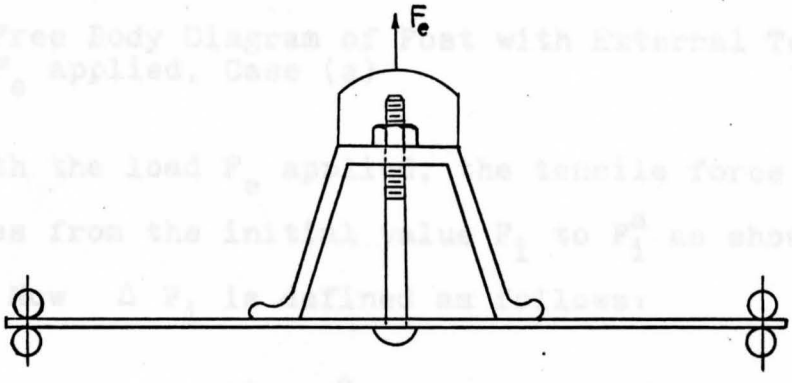

(a) Tensile Load

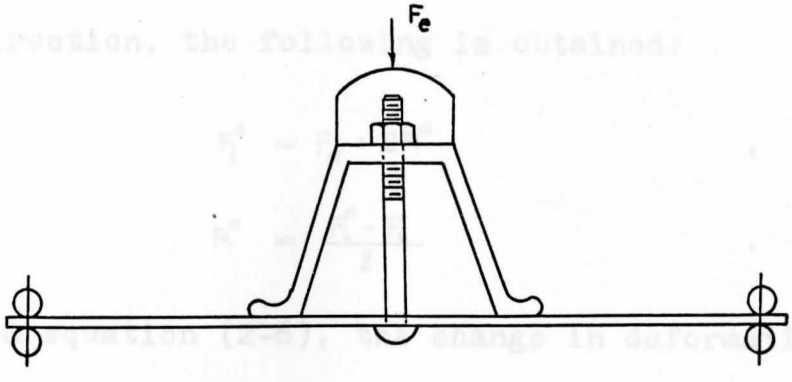

(b) Compressive Load

Figure 7 The External Load, F_e, Applied

Case (a) Tensile External Load

Since the bolt is initially in tension, it would have an increase in deformation amounting to $\Delta \delta_b$ as a result of the application of the tensile load F_e .

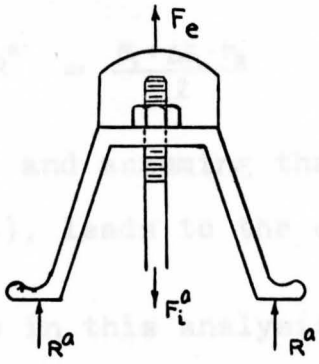

Figure 8 Free Body Diagram of Post with External Tensile Load F_e applied, Case (a)

With the load F_e applied, the tensile force in the bolt changes from the initial value F_i to F_i^a as shown in Figure 8. Now ΔF_i is defined as follows:

$$\Delta F_i = F_i^a - F_i \quad . \quad (2\text{-}12)$$

Using Figure 8 and considering static equilibrium in the vertical direction, the following is obtained:

$$F_i^a = F_e + 2R^a \quad , \quad (2\text{-}13)$$

or,

$$R^a = \frac{F_i^a - F_e}{2} \quad . \quad (2\text{-}14)$$

From equation (2-6), the change in deformation of the bolt can be expressed as

$$\Delta \delta_b = \frac{\Delta F_i}{K_b} \quad . \quad (2\text{-}15)$$

Substituting ΔF_i from equation (2-12) into equation (2-15) gives

$$\Delta \delta_b = \frac{F_i^a - F_i}{K_b} \quad . \quad (2\text{-}16)$$

Now, substituting equation (2-12) into equation (2-14) gives

$$R^a = \frac{F_i + \Delta F_i - F_e}{2} \quad . \quad (2\text{-}17)$$

Using equation (2-17) and assuming that $F_e \rangle \Delta F_i$ and comparing this to equation (2-4), leads to the conclusion that $|R^a| \langle |F_R|$.

The next step in this analysis was the determination of the maximum deflection at the mid-span of sign face section shown in Figure 9.

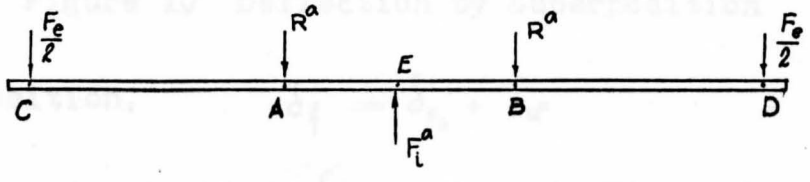

Figure 9 Free Body Diagram of the Sign Face with External Load F_e applied, Case (a)

The moment area method along with the superposition principal were then applied to sign face.

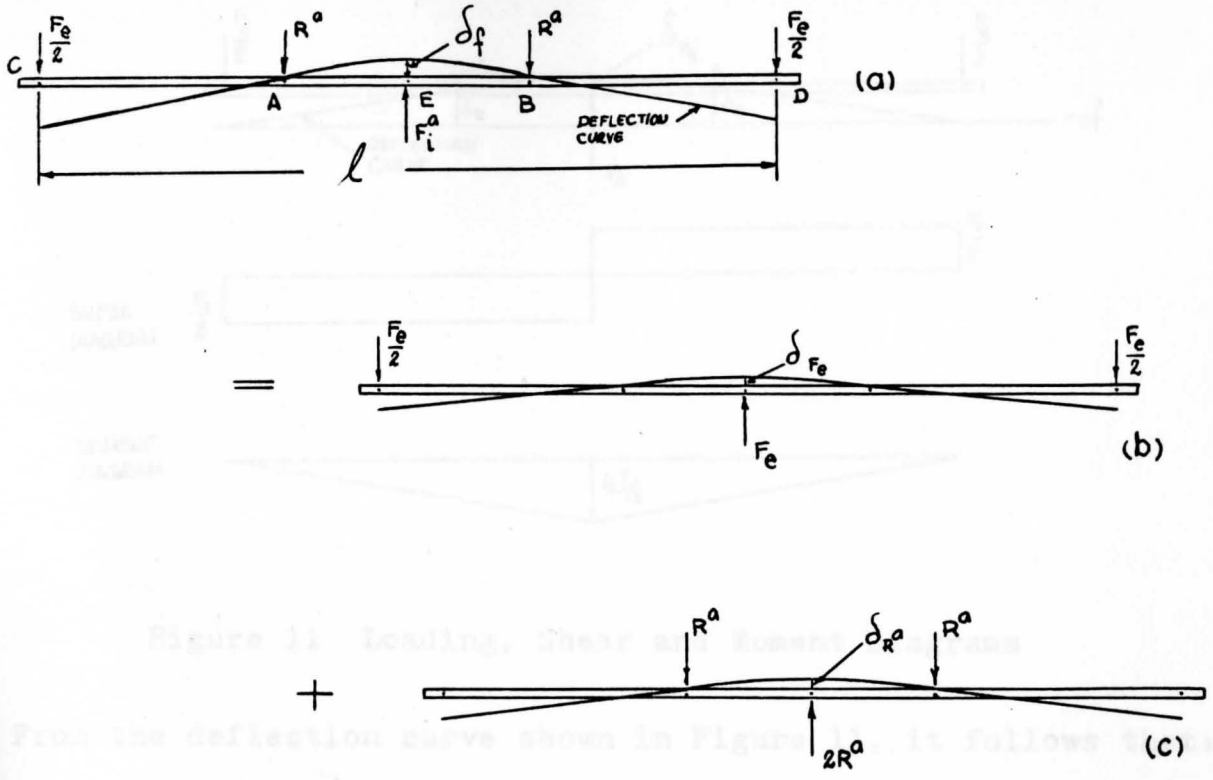

Figure 10 Deflection by Superposition

By superposition, $$\delta_f = \delta_{F_e} + \delta_{R^a} \quad . \quad (2\text{-}18)$$

In order to find δ_{F_e} as shown in Figure 10b, it was necessary to draw its moment diagram. Accordingly, drawn in Figure 11 are the loading, shear and moment diagrams treating the sign face as a simple beam with a concentrated center load of F_e.

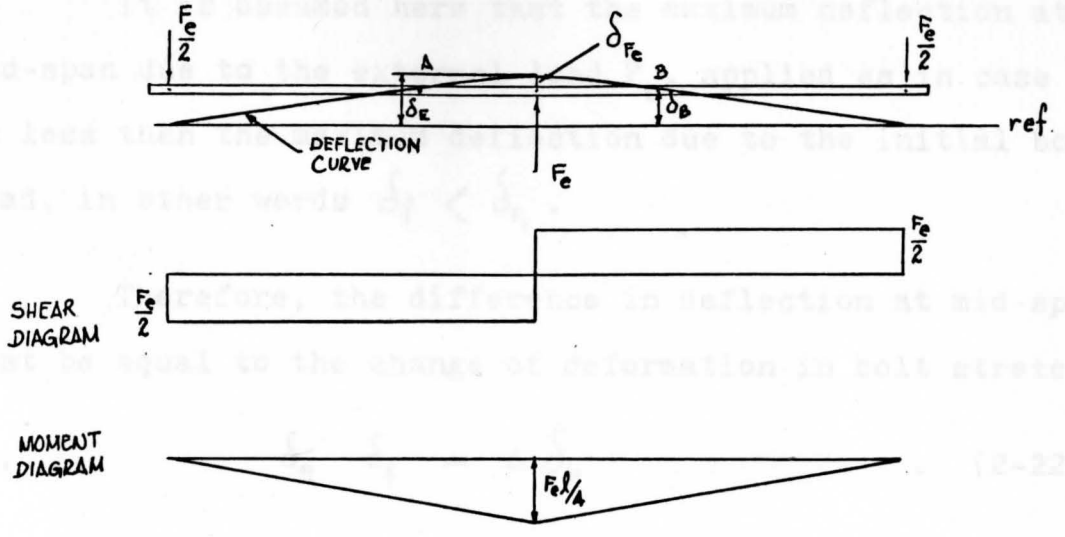

Figure 11 Loading, Shear and Moment Diagrams

From the deflection curve shown in Figure 11, it follows that:

$$\delta_{F_e} = \delta_E - \delta_B \quad ,$$

or,

$$\delta_{F_e} = \frac{F_e l^3}{48 E_{sf} I} - \frac{F_e\left(\frac{l}{2} - \frac{x}{2}\right)}{48 E_{sf} I}\left[3l^2 - 4\left(\frac{l}{2} - \frac{x}{2}\right)^2\right] \quad ,$$

$$\delta_{F_e} = \frac{F_e x^2 (3l - x)}{96 E_{sf} I} \quad ,$$

$$\delta_{F_e} = \frac{F_e}{K_{F_e}} \quad , \qquad (2\text{-}19)$$

where,

$$K_{F_e} = \frac{96 E_{sf} I}{x^2 (3l - x)} \quad .$$

Recognizing the similarity between Figures 10c and 6, it follows that:

$$\delta_{R^a} = \frac{R^a}{K_p} \quad . \qquad (2\text{-}20)$$

Now, substituting equations (2-19) and (2-20) into equation (2-18) gives:

$$\delta_f = \frac{F_e}{K_{F_e}} + \frac{R^a}{K_p} \quad . \qquad (2\text{-}21)$$

It is assumed here that the maximum deflection at mid-span due to the external load F_e, applied as in case (a) is less than the maximum deflection due to the initial bolt load, in other words $\delta_f < \delta_{F_i}$.

Therefore, the difference in deflection at mid-span must be equal to the change of deformation in bolt stretch,

or, $$\delta_{F_i} - \delta_f = \Delta \delta_b \quad . \quad (2\text{-}22)$$

Substituting equations (2-9), (2-16) and (2-21) into (2-22) gives:

$$\frac{F_R}{K_p} - \left(\frac{F_e}{K_{F_e}} + \frac{R^a}{K_p}\right) = \frac{F_i^a - F_i}{K_b} \quad ,$$

or, $$\frac{F_R - R^a}{K_p} - \frac{F_e}{K_{F_e}} = \frac{F_i^a - F_i}{K_b} \quad . \quad (2\text{-}23)$$

Substituting F_i^a from equation (2-13) into (2-23), and solving for R^a gives:

$$\frac{F_R - R^a}{K_p} - \frac{F_e}{K_{F_e}} = \frac{F_e + 2R^a - F_i}{K_b} \quad .$$

Since $F_i = 2F_R$, it follows that

$$\frac{F_R}{K_p} - \frac{R^a}{K_p} - \frac{F_e}{K_{F_e}} = \frac{F_e}{K_b} + \frac{2R^a}{K_b} - \frac{2F_R}{K_b} \quad ,$$

$$\frac{2R^a}{K_b} + \frac{R^a}{K_p} = \left[\left(\frac{1}{K_p} + \frac{2}{K_b}\right)F_R - \left(\frac{1}{K_{F_e}} + \frac{1}{K_b}\right)F_e\right] \quad ,$$

$$R^a = \frac{K_b K_p}{2K_p + K_b}\left[\left(\frac{K_b + 2K_p}{K_p K_b}\right)F_R - \left(\frac{K_b + K_{F_e}}{K_{F_e} K_b}\right)F_e\right] \quad ,$$

$$R^a = F_R - \frac{K_p}{K_{F_e}}\left(\frac{K_b + K_{F_e}}{2K_p + K_b}\right)F_e \quad . \quad (2\text{-}24)$$

If a sufficiently large F_e is applied in this case, the sign face will no longer be in contact with the edge of the post, or $R^a = 0$. Then from equation (2-24) a limiting value of F_e can be computed for the condition which results in $R^a = 0$; i.e.,

$$\left(F_e\right)_{limit} = \frac{K_{F_e}}{K_p}\left(\frac{2K_p + K_b}{K_b + K_{F_e}}\right) F_R \quad . \quad (2\text{-}25)$$

Now, from equation (2-13) and with $F_e \geqslant (F_e)_{limit}$,

$$F_i^a = F_e + 2(0) \quad ,$$

or,

$$= F_e \quad .$$

In this case then where F_e is increased beyond $(F_e)_{limit}$ and $R^a = 0$, the force in the bolt is equal to the applied force, F_e.

Case (b) External Compressive Load

When the load F_e is applied in compression as shown in Figure 12, the tensile force in the bolt changes from the initial value F_i to F_i^b.

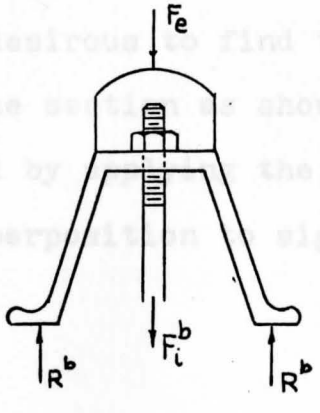

Figure 12 Free Body Diagram of Post with External Compressive Load F_e applied, Case (b)

Now, defining the change in bolt force as ΔF_i, it follows that:

$$\Delta F_i = F_i^b - F_i \quad . \quad (2\text{-}26)$$

Using Figure 12 and considering static equilibrium in the vertical direction, the following is obtained:

$$F_i^b = 2R^b - F_e \quad , \quad (2\text{-}27)$$

or,

$$R^b = \frac{F_i^b + F_e}{2} \quad . \quad (2\text{-}28)$$

Substituting ΔF_i from equation (2-26) into equation (2-15) gives

$$\Delta \delta_b = \frac{F_i^b - F_i}{K_b} \quad . \quad (2\text{-}29)$$

Now, substituting equation (2-26) into (2-28) gives

$$R^b = \frac{F_i + \Delta F_i + F_e}{2} \quad . \quad (2\text{-}30)$$

By comparing equation (2-30) to (2-4), leads to the conclusion that $|R^b| > |F_R|$.

It is next desirous to find the deflection at the mid-span of sign face section as shown in Figure 13 below. This is accomplished by applying the moment area method and the principal of superposition to sign face as outlined by Figure 14.

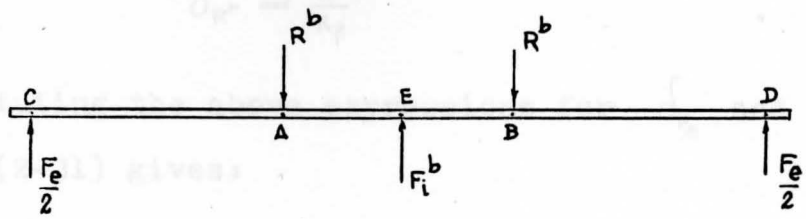

Figure 13 Free Body Diagram of the Sign Face with the External Load F_e applied, Case b

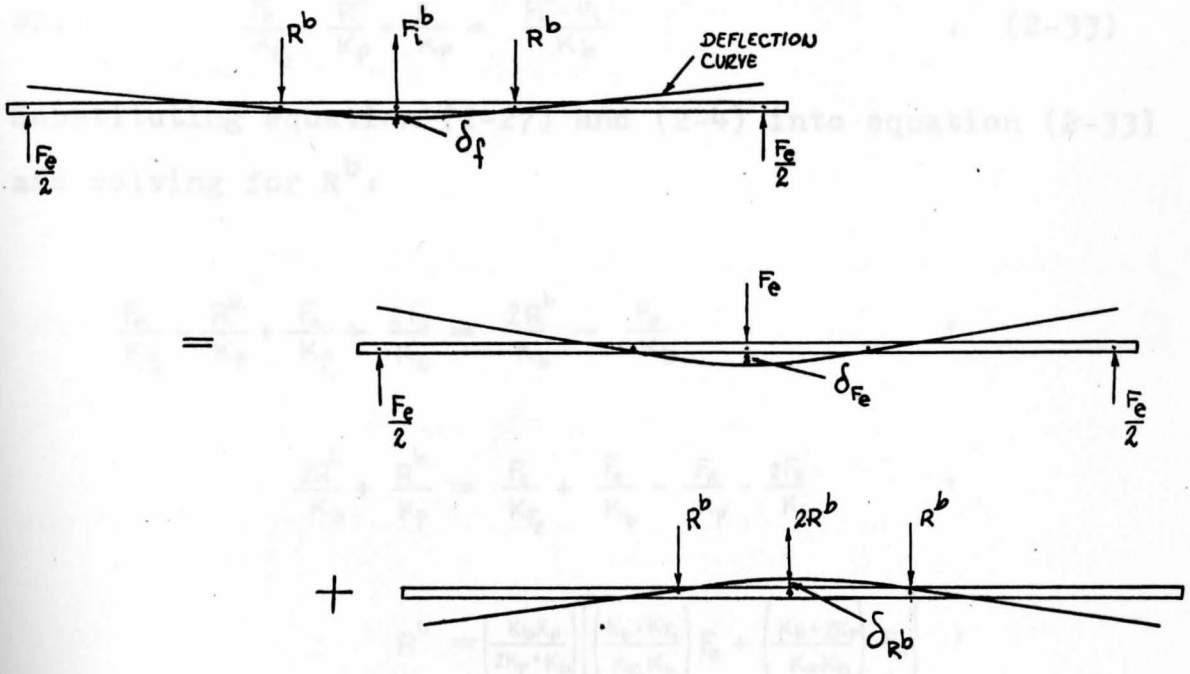

Figure 14 Deflection by Superposition

From the principal of superposition, it follows that:

$$\delta_f = \delta_{F_e} - \delta_{R^b} \qquad . \quad (2\text{-}31)$$

Using procedures similar to Case (a), the following expressions can be obtained for deflections:

$$\delta_{Fe} = \frac{F_e}{K_{Fe}} \quad ,$$

and $$\delta_{R^b} = \frac{R^b}{K_p} \quad .$$

By substituting the above expressions for δ_{Fe} and δ_{R^b} into equation (2-31) gives:

$$\delta_f = \frac{F_e}{K_{Fe}} - \frac{R^b}{K_p} \quad . \quad (2\text{-}32)$$

Then, the additional stretch in the bolt $\Delta\delta_b$ is equal to $\delta_f + \delta_{Fi}$, or $\Delta\delta_b = \delta_f + \delta_{Fi}$,

or, $$\frac{F_e}{K_{Fe}} - \frac{R^b}{K_p} + \frac{F_R}{K_p} = \frac{F_i^b - F_i}{K_b} \quad . \quad (2\text{-}33)$$

Substituting equation (2-27) and (2-4) into equation (2-33) and solving for R^b:

$$\frac{F_e}{K_{Fe}} - \frac{R^b}{K_p} + \frac{F_R}{K_p} + \frac{2F_R}{K_b} = \frac{2R^b}{K_b} - \frac{F_e}{K_b} \quad ,$$

$$\frac{2R^b}{K_b} + \frac{R^b}{K_p} = \frac{F_e}{K_{Fe}} + \frac{F_e}{K_b} - \frac{F_R}{K_p} - \frac{2F_R}{K_b} \quad ,$$

$$R^b = \left(\frac{K_b K_p}{2K_p + K_b}\right)\left[\left(\frac{K_b + K_{Fe}}{K_{Fe} K_b}\right) F_e + \left(\frac{K_b + 2K_p}{K_p K_b}\right) F_R\right] \quad ,$$

$$R^b = \frac{K_p}{K_{Fe}}\left(\frac{K_b + K_{Fe}}{2K_p + K_b}\right) F_e + F_R \quad . \quad (2\text{-}34)$$

Substituting equation (2-34) into (2-27) leads to the following expression for the bolt force F_i^b :

$$F_i^b = 2\frac{K_p}{K_{Fe}}\left(\frac{K_b + K_{Fe}}{2K_p + K_b}\right) F_e + 2F_R - F_e \quad ,$$

$$F_i^b = \left[2\frac{K_p}{K_{F_e}}\left(\frac{K_b + K_{F_e}}{K_b + 2K_p}\right) - 1 \right] F_e + 2F_R \quad . \quad (2\text{-}35)$$

Stress in the Sign Face

The objective of the next section of this analysis is to develop expressions for the maximum stress in the sign face. The first step will determine the stress resulting from the initial preload F_i caused by tightening the bolts.

Referring to Figure 6, the maximum stress at the mounting hole area, point E, can be determined by using the simple bending stress equation:

$$\sigma = \frac{Mc}{I} \quad . \quad (2\text{-}36)$$

From Figure 6, the maximum bending moment occurs at point E and can be written as:

$$M_E = \frac{F_R \alpha}{2} \quad . \quad (2\text{-}37)$$

Substituting equation (2-5) into (2-37) gives

$$M_E = \frac{T}{2\mu D} \cdot \frac{\alpha}{2} \quad . \quad (2\text{-}38)$$

From the bending stress equation, the largest flexure stress occurs in the outer fibers of the sign face. It therefore follows that

$$c = \frac{t}{2} \quad . \quad (2\text{-}39)$$

Since there is the hole at point E, the inertia will be reduced by substracting the hole's diameter from the width dimension; i.e.,

$$I = \frac{(b-2r)t^3}{12} \quad . \quad (2\text{-}40)$$

Substituting equations (2-39) and (2-40) into (2-36) gives

$$\sigma_E = \frac{T\alpha}{4\mu D} \cdot \frac{t}{2} \cdot \frac{12}{(b-2r)t^3} \quad ,$$

$$= \frac{3T\alpha}{2\mu D(b-2r)t^2} \quad . \quad (2\text{-}41)$$

The maximum bending stress at this point, including stress concentration effects, can be obtained by multiplying equation (2-41) by the stress concentration factor, K_t.

It is next desirous to compute the stresses resulting from the application of an external tensile load as shown in Figure 7(a). Referring to Figure 9, the bending moments at points A and E can be determined by taking moments of forces about points A and E respectively. Therefore,

$$\circlearrowleft + \quad M_A = \frac{F_e}{4}(l-x) \quad , \quad (2\text{-}42)$$

$$\circlearrowleft + \quad M_E = \frac{F_e l}{4} + \frac{R^a x}{2} \quad . \quad (2\text{-}43)$$

Substituting R^a from equation (2-24) into (2-43) gives

$$\circlearrowleft + \quad M_E = \frac{F_e l}{4} + \left[F_e - \frac{K_p}{K_{F_e}} \left(\frac{K_b + K_{F_e}}{K_b + 2K_p} \right) F_e \right] \frac{x}{2} \quad . \quad (2\text{-}44)$$

But $(F_e)_{limit}$ can be calculated by equation (2-25) and known that if $F_e \geqslant (F_e)_{limit}$ then $F_i^a = F_e$ since $R^a = 0$, therefore the moment at E will be

$$\circlearrowleft + \quad M_E = \frac{F_e}{2} \cdot \frac{l}{2} \quad . \quad (2\text{-}45)$$

Knowing the bending moments at points A and E, the bending stresses at these points can be obtained by using

equation (2-36). Therefore,

$$\sigma_A = \frac{F_e}{4}(l-x)\cdot\frac{c}{I_A} \quad . \quad (2\text{-}46)$$

and $$\sigma_E = \left[\frac{F_e l}{4} + \left\{F_R - \frac{K_p}{K_{Fe}}\left(\frac{K_b + K_{Fe}}{K_b + 2K_p}\right)F_e\right\}\frac{x}{l}\right]\frac{c}{I_E} \quad ,$$

when $F_e < (F_e)_{limit}$, (2-47)

or, $$\sigma_E = \frac{F_e l}{4}\cdot\frac{c}{I_E} \quad , \text{when } F_e \geqslant (F_e)_{limit} \quad . \quad (2\text{-}48)$$

where, $c = \frac{t}{2}$,

$I_A = \frac{bt^3}{12}$,

$I_E = \frac{(b-2r)t^3}{12}$.

The maximum bending stress at point E including stress concentration effects can be obtained by multiplying equations (2-47) and (2-48) by the stress concentration factor, K_t.

The following step will determine the stresses resulting from the application of an external compressive load as shown in Figure 7(b). Referring to Figure 13, the moment at points A and E can be determined by taking moments of forces about points A and E respectively. It follows that:

$$(+ \qquad M_A = -\frac{F_e}{4}(l-x) \quad , \quad (2\text{-}49)$$

$$(+ \qquad M_E = -\frac{F_e l}{4} + \frac{R x}{l} \quad . \quad (2\text{-}50)$$

Substituting equation (2-34) into (2-50), results

$$M_E = -\frac{F_e l}{4} + \left[\frac{K_p}{K_{Fe}}\left(\frac{K_b + K_{Fe}}{2K_p + K_b}\right)F_e + F_R\right]\frac{x}{2} \quad . \quad (2\text{-}51)$$

Therefore, the bending stress at points A and E can be obtained by using equation (2-36), leads to

$$\sigma_A = \frac{F_e}{4}\left(\ell - x\right)\frac{c}{I_A} \quad , \quad (2\text{-}52)$$

and

$$\sigma_E = \left[-\frac{F_e \ell}{4} + \left\{\frac{K_p}{K_{F_e}}\left(\frac{K_b + K_{F_e}}{K_b + 2K_p}\right)F_e + F_R\right\}\frac{x}{\ell}\right]\frac{c}{I_E} \quad , \quad (2\text{-}53)$$

where,

$$c = \frac{t}{2} \quad ,$$

$$I_A = \frac{bt^3}{12} \quad ,$$

$$I_E = \frac{(b-2r)t^3}{12} \quad .$$

The maximum bending stress at point E including stress concentration effects can be obtained by multiplying equation (2-53) by the stress concentration factor, K_t.

Stress in the Bolt

The objective of this part of analysis is to develop expressions for the tensile stress normal to the bolt section. There are two cases which are involved in this project. The first case is to determine the tensile stress in the bolt resulting from the application of an external tensile load as shown in Figure 7(a). The tensile stress can be expressed as

$$\sigma_b = \frac{F_i^a}{A_b} \quad . \quad (2\text{-}54)$$

Before going to substitute F_i^a into equation (2-54), a limiting value of F_e will be computed by using equation (2-25). Therefore, the required tensile stress can be determined by the

following equations:

$$\sigma_b = \frac{F_e}{A_b} \quad , \text{ for } F_e \gg (F_e)_{limit}. \qquad (2\text{-}55)$$

$$\text{or, } \sigma_b = \frac{\left[1 - \left(\frac{2K_p}{K_{Fe}}\right)\left(\frac{K_b + K_{Fe}}{K_b + 2K_p}\right)\right] F_e + 2F_R}{A_b} \quad , \text{ for } F_e < (F_e)_{limit}. \qquad (2\text{-}56)$$

The second case deals with the external compressive load applied to the sign-post connection. Thus, the tensile stress normal to the bolt section can be expressed as:

$$\sigma_b = \frac{F_i^b}{A_b} \quad . \qquad (2\text{-}57)$$

Substituting equation (2-35) into (2-57) gives

$$\sigma_b = \frac{\left[2\,\frac{K_p}{K_{Fe}}\left(\frac{K_b + K_{Fe}}{K_b + 2K_p}\right) - 1\right] F_e + 2F_R}{A_b} \quad . \qquad (2\text{-}58)$$

Equation (2-35) which gives the theoretical value of bolt force was obtained by using simple beam theory. When specific values were substituted into this equation, a poor correlation with experimental results was obtained as will be shown in the next chapter. In order to improve this correlation, and in observing the deformation of the sign face near the mounting bolt, it was decided to use plate theory for the deflection of the sign face under the bolt's load.

Accordingly, equations (2-34) and (2-35) were corrected in this fashion and the sign face was considered to be a flat plate in the mounting hole area under the external compressive load F_e, (case b) as shown in Figure 15 below. It will be

seen that the deflection at the mounting hole using plate theory will be larger than that resulting from a concentrated load at mid-span of a simply supported beam.

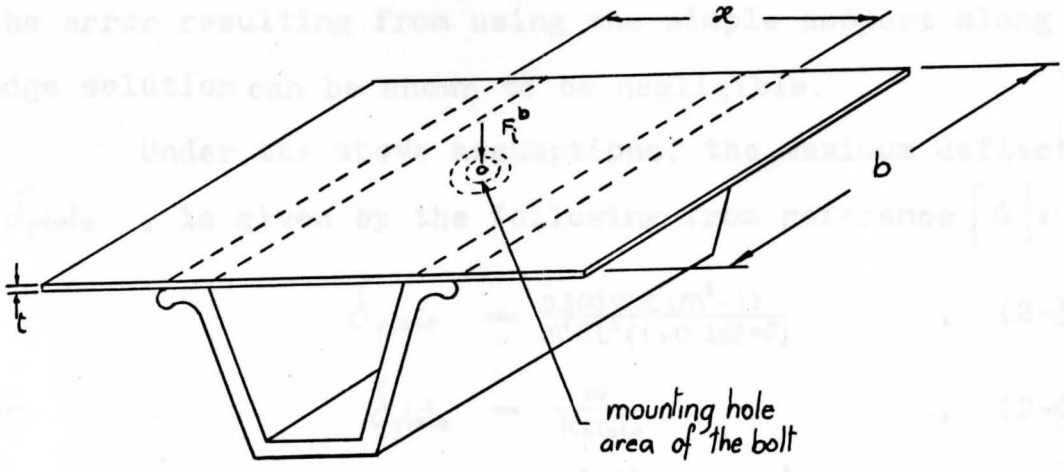

Figure 15 Concentrate Load applied at the Center of the Mounting Hole Area

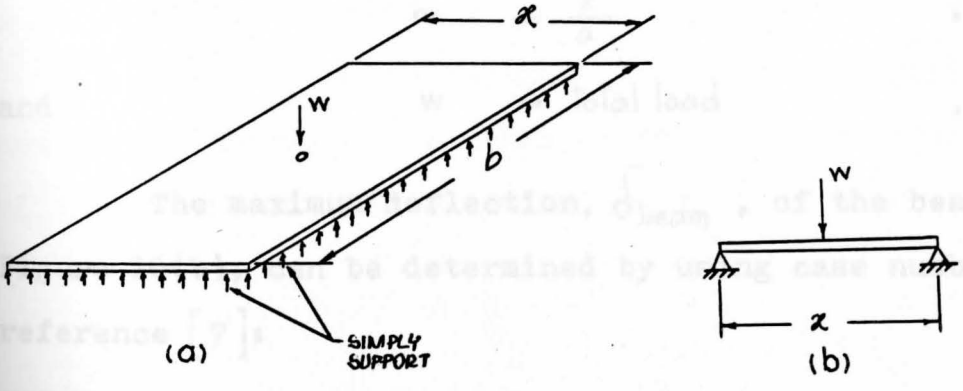

Figure 16 (a) Concentrated Load at the Mid-Point of the Plate

(b) Concentrated Load at the Mid-Span of the Beam

In using plate theory, it was assumed that the plate was simply supported along all edges as shown in Figure 16(a). With a concentrated load at the center and with this type of a support structure, the deflection under the load can be

found from reference [6] as case No. 36. Although the sign face is not supported along the short edges, of length x, it can be shown that for plates with b $\gg$ x as is the case here, the error resulting from using the simple support along all edge solution can be shown to be negligible.

Under the above assumptions, the maximum deflection, δ_{plate}, is given by the following from reference [6]:

$$\delta_{plate} = \frac{0.203 W x^2 (m^2-1)}{m^2 E t^3 (1+0.462\alpha^2)} \quad , \quad (2\text{-}59)$$

or,
$$\delta_{plate} = \frac{W}{K_{plate}} \quad , \quad (2\text{-}60)$$

where,
$$K_{plate} = \frac{m^2 E t^3 (1+0.462\alpha^2)}{0.203\, x^2 (m^2-1)} \quad , \quad (2\text{-}61)$$

$$m = \frac{1}{\nu} \quad ,$$

$$\alpha = \frac{x}{a} \quad ,$$

and
$$W = \text{total load} \quad .$$

The maximum deflection, δ_{beam}, of the beam at mid-span, Figure 16(b), can be determined by using case number 8 from reference [7]:

Therefore,
$$\delta_{beam} = \frac{W x^3}{48 E I} \quad , \quad (2\text{-}62)$$

or,
$$\delta_{beam} = \frac{W}{K_B} \quad , \quad (2\text{-}63)$$

where,
$$K_B = \frac{48 E I}{x^3} \quad , \quad (2\text{-}64)$$

and
$$I = \frac{(b-2r) t^3}{12} \quad .$$

Letting b = 10", x = $3\frac{1}{2}$", t = 0.1", 2r = $\frac{3}{8}$", E = 10 x 10^6 psi., and ν_{Al} = 0.33, and substituting these

typical values into equations (2-59) and (2-62), results in

$$\delta_{plate} = \frac{W}{0.4544\times10^{4}} \quad , \qquad (2\text{-}65)$$

and $$\delta_{beam} = \frac{W}{0.8979\times10^{4}} \quad . \qquad (2\text{-}66)$$

Dividing equation (2-65) by (2-66):

$$\frac{\delta_{plate}}{\delta_{beam}} = \frac{0.8979}{0.4544} \quad ,$$

$$= 1.976 \quad ,$$

or, $$\delta_{plate} = 1.976\,\delta_{beam} \quad .$$

It is thus seen that the maximum deflection of the plate is greater than the maximum deflections of the beam. Therefore, the stiffness constant of the plate, K_{plate}, is greater than the stiffness constant of the beam, K_{beam}.

The stiffness constant, K_p, used in equations (2-34) and (2-35) should now be changed to be the stiffness constant of the plate. Equation (2-32) can then be rewritten as

$$\delta_f = \frac{F_e}{K_{F_e}} - \frac{2R^b}{K_{plate}} \quad , \qquad (2\text{-}67)$$

and equation (2-33) will be

$$\frac{F_e}{K_{F_e}} - \frac{2R^b}{K_{plate}} + \frac{2F_R}{K_{plate}} = \frac{F_i^b - F_i}{K_b} \quad . \qquad (2\text{-}68)$$

Substituting equation (2-27) into (2-68) and solving for R^b gives:

$$\frac{F_e}{K_{F_e}} - \frac{2R^b}{K_{plate}} + \frac{2F_R}{K_{plate}} = \frac{2R^b}{K_b} - \frac{F_e}{K_b} - \frac{2F_R}{K_b} \quad ,$$

then, $$2R^b = \frac{K_{plate}}{K_{F_e}}\left(\frac{K_b + K_{F_e}}{K_b + K_{plate}}\right)F_e + 2F_R \quad . \qquad (2\text{-}69)$$

Substituting (2-69) into (2-27) gives

$$F_i^b = \left[\frac{K_{plate}}{K_{Fe}}\left(\frac{K_b + K_{Fe}}{K_b + K_{plate}}\right) - 1\right] F_e + 2F_R \quad . \quad (2\text{-}70)$$

Finally, the tensile stress in the bolt, equation (2-57), can be rewritten as

$$\sigma_b = \frac{\left[\frac{K_{plate}}{K_{Fe}}\left(\frac{K_b + K_{Fe}}{K_b + K_{plate}}\right) - 1\right] F_e + 2F_R}{A_b} \quad , \quad (2\text{-}71)$$

and the average stress at point E will be given by:

$$\sigma_E = \left[-\frac{F_e \ell}{4} + \left\{\frac{K_{plate}}{K_{Fe}}\left(\frac{K_b + K_{Fe}}{K_b + K_{plate}}\right)\frac{F_e}{2} + F_R\right\}\frac{\ell}{2}\right]\frac{c}{I_E} \quad . \quad (2\text{-}72)$$

CHAPTER III

THE MEASUREMENT OF EXPERIMENTAL STRESSES IN THE BOLT AND SIGN FACE

3.1 Introduction

The objective of this part of the project is to find the distribution of stresses around the hole, i.e., along the centerline passing through the holes. The stresses develop when the sign face is subjected to the initial preload F_i, in conjunction with the external tensile-type load and the external compressive load. In order to determine the stresses at any point in the sign face, it is necessary to employ a strain gage to measure the surface strains directly at the point in question. Thus, the conversion from the strains to the stresses can be achieved by employing the stress-strain relationships of Hooke's Law.

In this chapter, the experimentation conducted to measure the strain readings in the bolt is also described; in other words, the study involves:

1. the relationship between the tensile force in the bolt and its corresponding strain-gage reading; and,
2. the relationship between the tightening torque applied to the bolt nut and the corresponding strain-gage reading in the bolt.

The data so obtained will be utilized to determine the relationship between tensile force in the bolt and tightening torque. Moreover, this relationship can be used to determine the coefficient of friction between the bolt and sign. Also, the relationship between the tensile stress in the bolt and the external tensile and compressive applied loads can be obtained.

In the following sections of this chapter, three specific example problems are presented for the purpose of comparing the experimental results with theory. An average bending stress was determined from the measured distribution of strains (or stresses) acting along the centerline of the face near the bolt hole and compared to a theoretical average. In the first example, the face was subjected to an initial preload, F_i, caused by tightening the bolts and, the theoretical average was obtained by using equation (2-41). The face was subjected to an external-tensile load in the second example and, the theoretical average was obtained by using equation (2-47) or (2-48). In the third example, the face was subjected to an external compressive load and, the theoretical average was obtained by using equation (2-72).

In the last section of this chapter, example problems are presented that compare the tensile stress, as determined by the measured strain in the bolt, with the theoretical tensile stress obtained by using equations (2-55), (2-56) and (2-71). For the purpose of these analyses, the face was stressed by either a compressive or tensile-type load.

3.2 Stress Distribution in the Sign Face after the Bolt has been tightened

This section involves the determination of the distribution of stresses near the hole along the x axis of the sign face as shown in Figure 17. The experimentation is conducted by tightening the bolts to some known torque level and measuring the resulting surface strains in the y direction, near hole B, along the x axis. Measurement of the surface strains was accomplished by employing four strain gages along with strain gage instrumentation. The gages were bonded directly to the surface of the sign face, as shown in Figure 17.

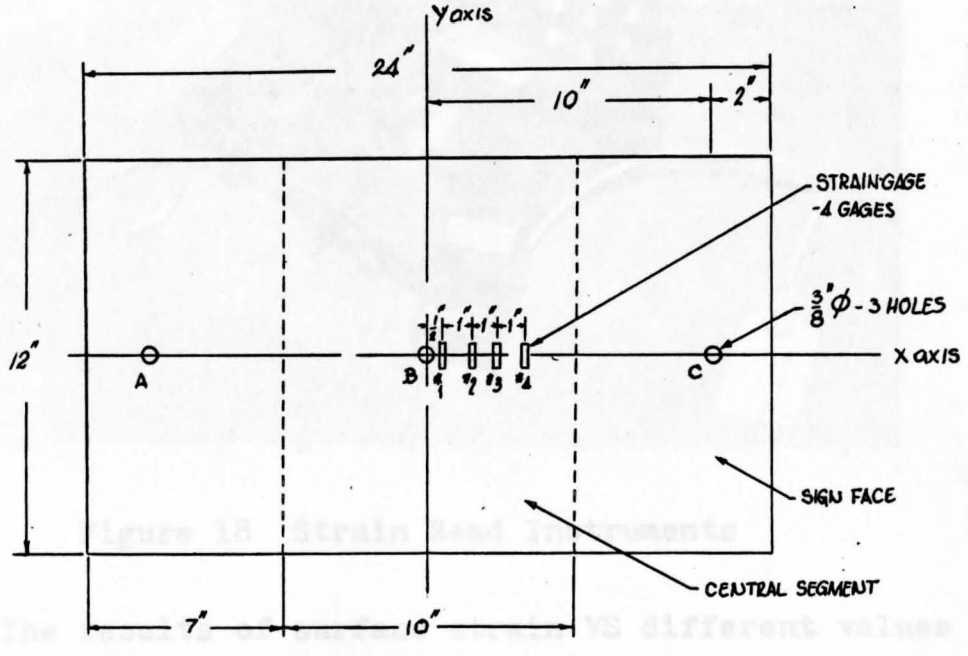

Figure 17 The Gages were bonded to the Sign Face.

The strain gages which were employed to accomplish this task have the following specifications:

Gage type	:	CEA - 13 - 250UW - 120
Resistance in ohms	:	120.0 $\pm$ 0.3%
Gage factor at 75 F	:	2.095 $\pm$ 0.5%
K_t	:	+0.3%

The strain signal conditioning and readout instruments used were the V/E 11 strain indicator with auxiliary units V/E - 12; V/E - 14 and 11 - A6 adaptor manufactured by Vishay Research & Education, as shown schematically in Figure 18.

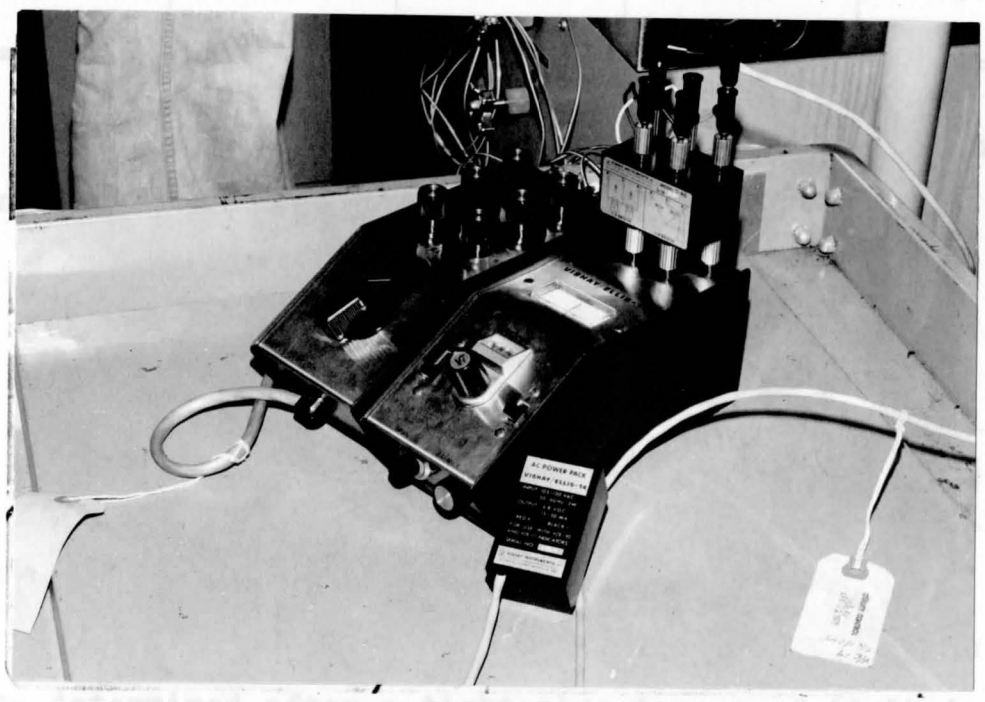

Figure 18 Strain Read Instruments

The results of surface strain VS different values of the tightening torque are presented in Table 1.

TABLE 1

SURFACE STRAINS IN THE SIGN FACE VS BOLT TIGHTENING TORQUE

Tightening Torque (lb-in.)	Strain Gage #1 μin/in	#2 μin/in	#3 μin/in	#4 μin/in
60	5020	2276	1174	706
80	5242	2410	1222	724
100	6054	2792	1418	830

The stresses can be computed from strains by employing the stress-strain relationship from Hooke's Law; i.e.,

$$\frac{\text{stress}}{\text{strain}} = \text{modulus of elasticity} \quad ,$$

or,
$$\frac{\sigma}{\epsilon} = E \quad . \quad (3\text{-}1)$$

For Aluminum 6063 - T6; the modulus of elasticity is approximately 10×10^6 psi.

Using (3-1), the stresses, for example, at gage No. 1 can be determined after a tightening torque of 60 lb-in. as:

$$\sigma = E\epsilon$$

or,
$$\sigma = 10 \times 10^6 \times \frac{5020}{10^6} \quad \text{psi}$$

$$\sigma = 50{,}200 \quad \text{psi} \quad .$$

Therefore, the stresses are calculated from the strains in Table 1, and are shown respectively in Table 2. All the stresses in this case are compressive stress.

TABLE 2

SURFACE STRESSES IN THE SIGN FACE VS BOLT TIGHTENING TORQUE

Tightening Torque (lb-in.)	Stresses #1 (psi)	#2 (psi)	#3 (psi)	#4 (psi)
60	50200	22760	11740	7060
80	52420	24100	12220	7240
100	60540	27920	14180	8300

Now, the average stress for each torque can be obtained by employing the mean value theorem. This can be achieved by determining the area under the curve obtained by plotting the distribution of stresses as a function of position along the x axis and dividing this area by the distance involved in the plot. The following example shows the calculation of the area under curve, when the distribution of stresses is plotted as a function of position along the x axis of the sign face for a tightening torque of 60 lb-in.; refer to Figure 19.

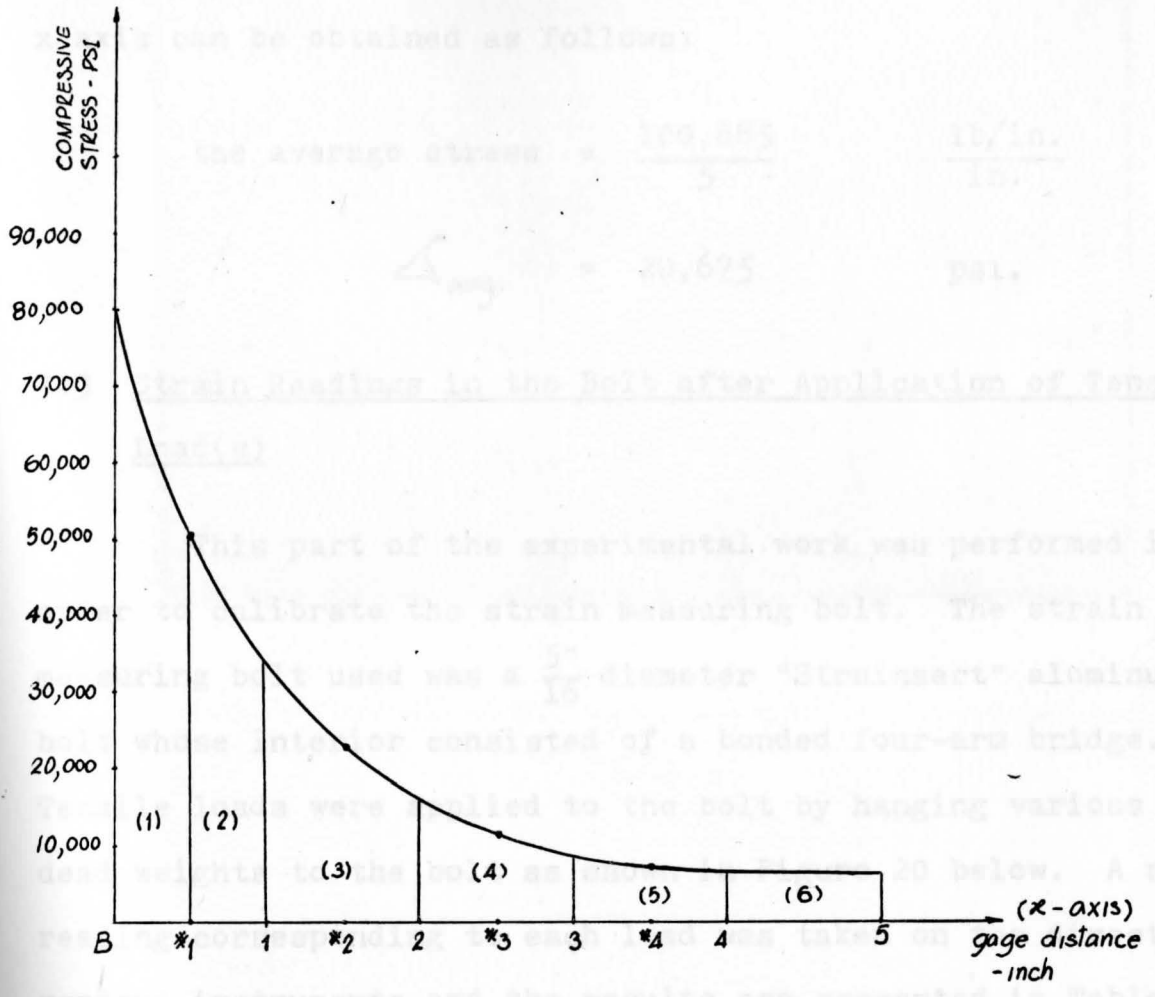

Figure 19 Distribution of Stresses along the x Axis

Area (1) : $\frac{1}{2} \times \frac{1}{2} \times (80{,}000 + 50{,}000)$

Area (2) : $\frac{1}{2} \times \frac{1}{2} \times (50{,}000 + 32{,}500)$

Area (3) : $1 \times \frac{1}{2} \times (32{,}500 + 16{,}000)$

Area (4) : $1 \times \frac{1}{2} \times (16{,}000 + 9{,}000)$

Area (5) : $1 \times \frac{1}{2} \times (9{,}000 + 6{,}000)$

Area (6) : $1 \times 6{,}000$

Summing areas 1 through 6 above, gives a total area of 103,375 lb/in.

Therefore, the average stress about hole B along the x axis can be obtained as follows:

$$\text{the average stress} = \frac{100{,}685}{5} \quad \frac{\text{lb/in.}}{\text{in.}}$$

$$\sigma_{avg.} = 20{,}675 \quad \text{psi.}$$

3.3 Strain Readings in the Bolt after Application of Tensile Load(s)

This part of the experimental work was performed in order to calibrate the strain measuring bolt. The strain measuring bolt used was a $\frac{5"}{16}$ diameter "Strainsert" aluminum bolt whose interior consisted of a bonded four-arm bridge. Tensile loads were applied to the bolt by hanging various size dead weights to the bolt as shown in Figure 20 below. A strain reading corresponding to each load was taken on the direct-readout instruments and the results are presented in Table 3. The readout instruments used for this part were the V/E 11, V/E 12 and V/E 14. In this experiment, the applied tensile load was gradually increased by the same increment for each reading.

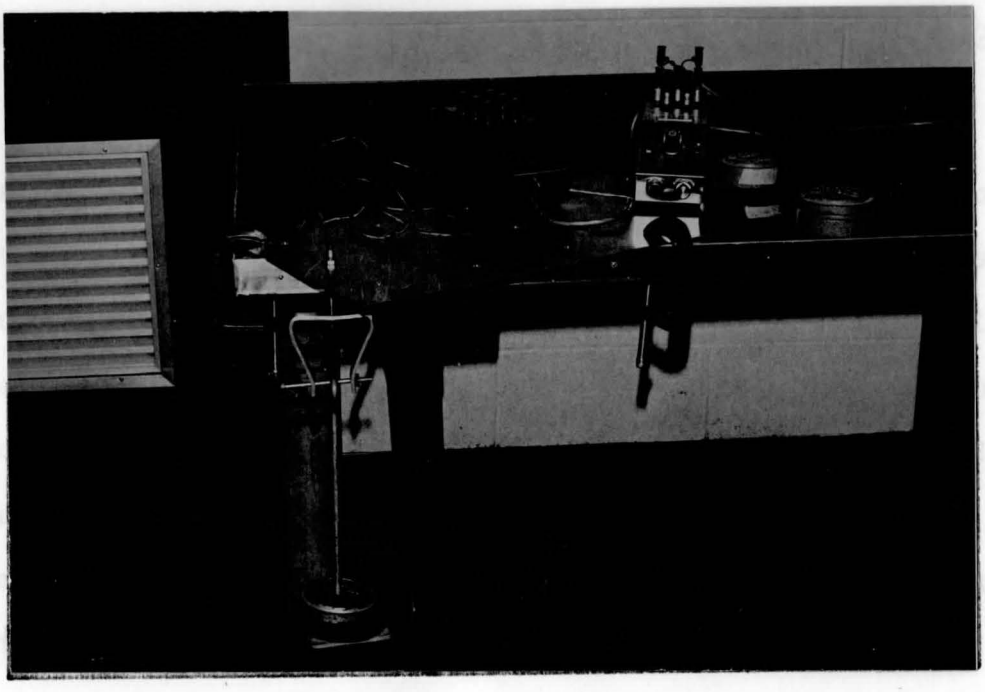

Figure 20 Photograph of the Tensile Load applied to the Bolt

TABLE 3

STRAIN READINGS IN THE BOLT VS APPLIED TENSILE LOADS

LOAD (lb)	STRAIN READINGS
10	170
15	264
20	356
25	456
30	556
35	656
40	756
45	856
50	954
55	1030

3.4 Strain Readings in the Bolt after Tightening the Bolt Nut

This section involves the acquisition of strain readings in the bolt after the bolt has been tightened by various torques. The same "Strainsert" bolt was used as in Section 3.3, and the same read-out instruments were employed. Figure 21 shows all the instruments employed in this experiment. The bolt was tightened by a calibrated torque wrench and the tightening torques were gradually increased by the same increment for each bolt strain reading. The experimental results for this test are presented in Table 4.

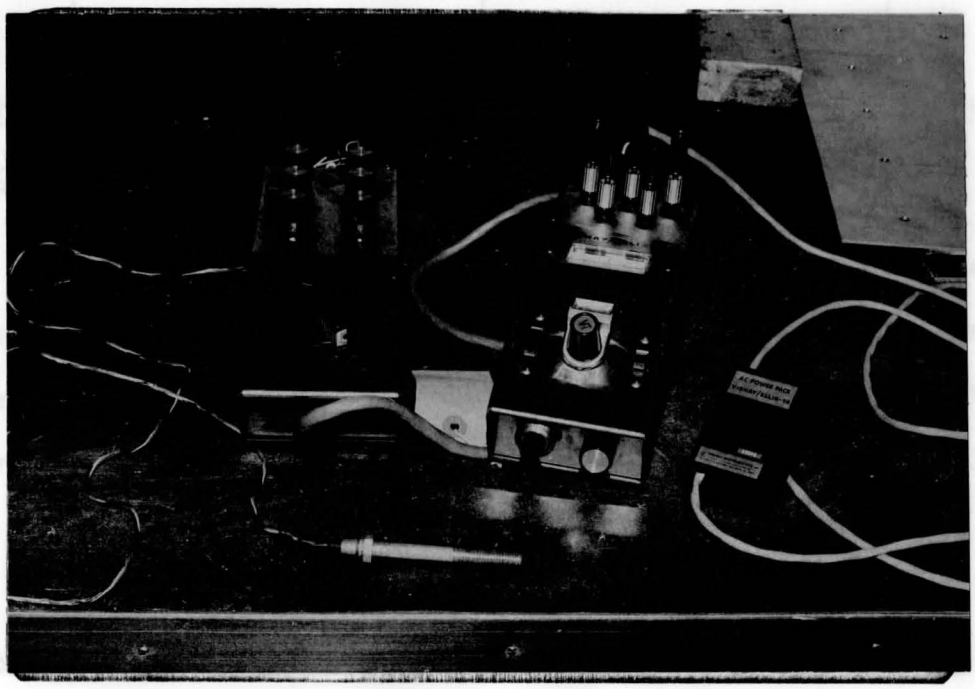

Figure 21 Photograph of a "Strainsert" Bolt and Strain Readout Instruments

TABLE 4

STRAIN READINGS IN THE BOLT VS BOLT TIGHTENING TORQUE

TORQUE (lb-in.)	STRAIN READINGS
10	1078
20	2097
30	3526
40	5453
50	7754
60	9456

3.5 The Relationship between the Bolt Tension and Tightening Torques

The objective of this section is to determine the tensile force in the bolt after the bolt has been tightened by using the experimental data obtained in the previous two sections. Also, the coefficient of thread and nut friction can be established once this relationship is obtained.

The strain readings are plotted as a function of tensile load by using the results from Table 3, and are shown in Figure 22. The bolt strain readings are plotted as a function of the tightening torque by using the results tabulated in Table 4, and are shown in Figure 23.

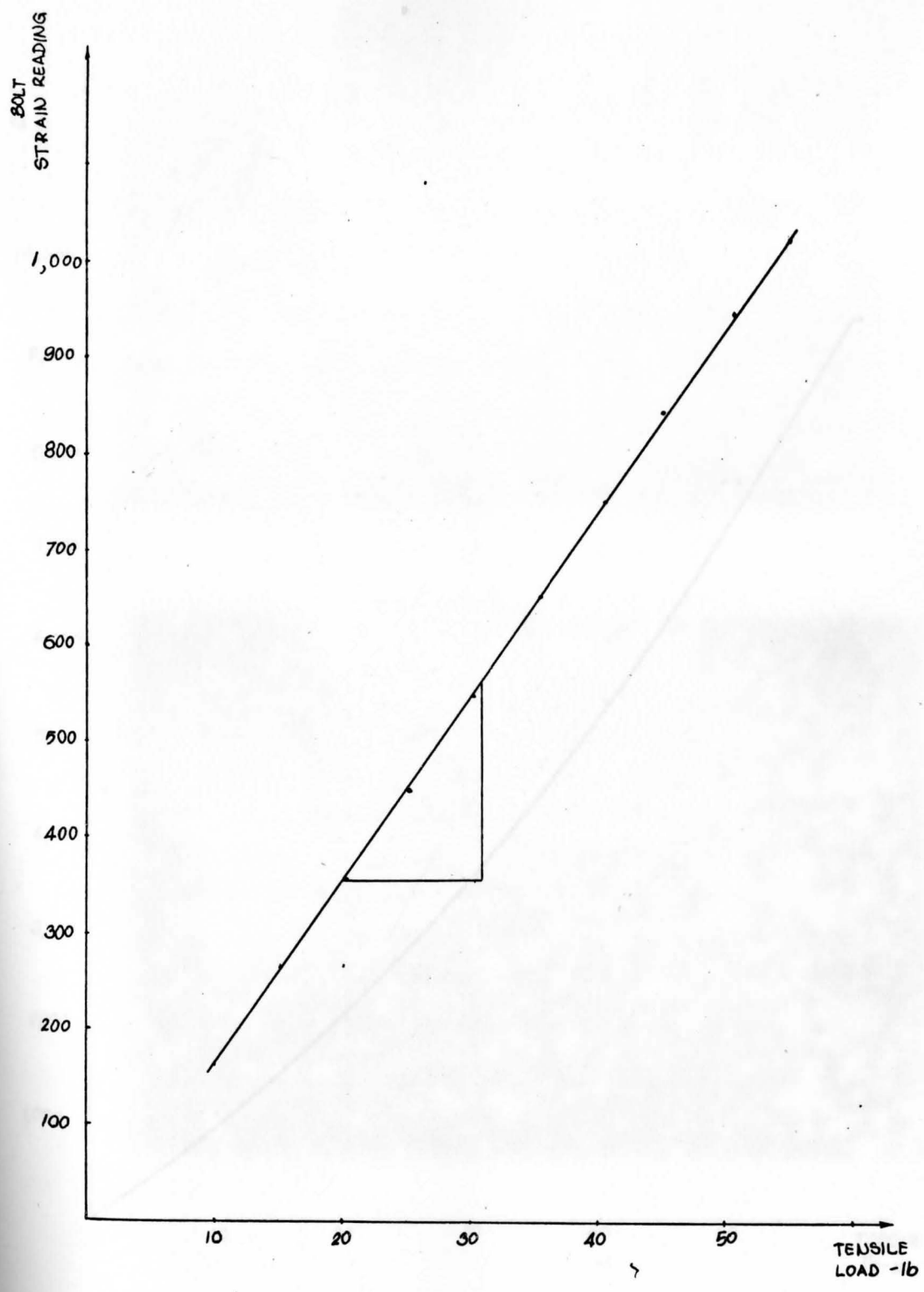

Figure 22 Bolt Strain Readings as a Function of Tension

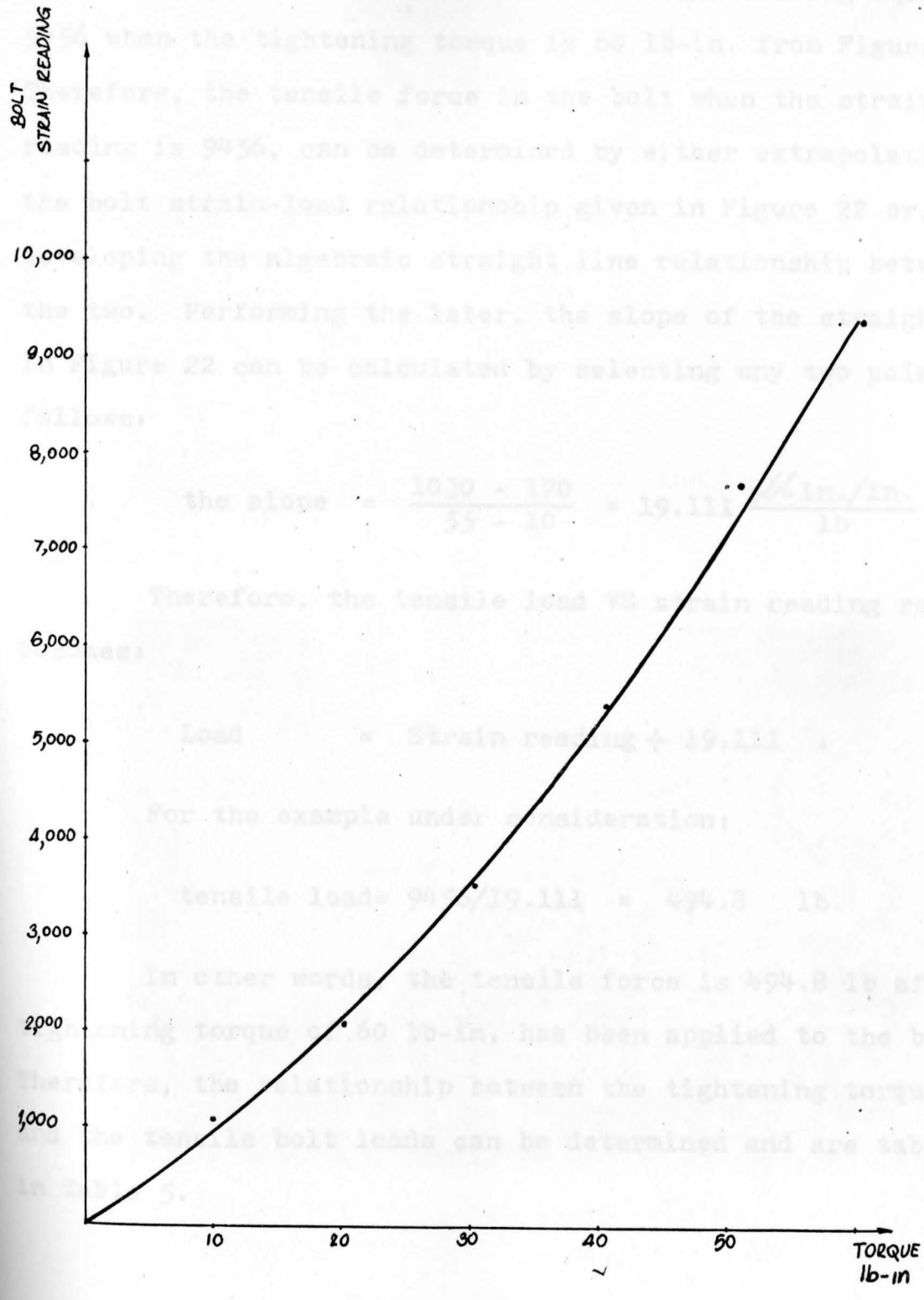

Figure 23 Bolt Strain Readings as a Function of Tightening Torque

It can be seen that the bolt strain reading equals 9456 when the tightening torque is 60 lb-in. from Figure 23. Therefore, the tensile force in the bolt when the strain reading is 9456, can be determined by either extrapolating the bolt strain-load relationship given in Figure 22 or, by developing the algebraic straight line relationship between the two. Performing the later, the slope of the straight-line in Figure 22 can be calculated by selecting any two points as follows:

$$\text{the slope} = \frac{1030 - 170}{55 - 10} = 19.111 \frac{\mu \text{in./in.}}{\text{lb}}$$

Therefore, the tensile load VS strain reading relationship becomes:

$$\text{Load} = \text{Strain reading} \div 19.111 \ .$$

For the example under consideration;

$$\text{tensile load} = 9456/19.111 = 494.8 \text{ lb.}$$

In other words, the tensile force is 494.8 lb after a tightening torque of 60 lb-in. has been applied to the bolt. Therefore, the relationship between the tightening torques and the tensile bolt loads can be determined and are tabulated in Table 5.

TABLE 5

TENSILE LOAD ON BOLT VS BOLT TIGHTENING TORQUE

TIGHTENING TORQUE (lb-in.)	BOLT-LOAD (lb)
10	56.40
20	108.80
30	184.50
40	285.33
50	405.70
60	494.80

By considering the relationship between the tensile bolt load and the tightening torque from Table 5, it can be seen that the constant μ, relating bolt force with torque, described in Chapter II can be determined as follows:

From equation (2-2): $T = \mu DF_i$,

or, $$\mu = \frac{T}{DF_i} \quad . \quad (3\text{-}2)$$

Referring to Table 5, the tightening torque 10 lb-in. results in a tensile force of 56.40 lb, and by substituting these two values into equation (3-2), yields

$$\mu = 0.567 \quad .$$

Following this procedure, the values of all the coefficients VS 10 lb-in. torque increments are tabulated in Table 6. Thus, an approximate μ coefficient for the bolt can be determined by using the average value of Table 6.

TABLE 6

COEFFICIENT OF THREAD FRICTION

TORQUE (lb-in.)	BOLT-FORCE (lb)	μ
10	56.40	0.567
20	108.80	0.588
30	184.50	0.520
40	285.33	0.448
50	405.70	0.394
60	494.80	0.388

The average μ , from Table 6 is equal to 0.48, and now equation (2-2) can be rewritten as:

$$T = 0.48\ DF_i \quad . \quad (3\text{-}3)$$

The next step of this section involves the determination of the average stress along the x axis of the sign face near hole B, from the initial preload F_i caused by tightening the bolt. The following example will show the calculation of the average stress by using equations(2-41) and (3-3).

Example

When the bolt has been tightened to 60 lb-in. torque and for a bolt diameter of $\frac{5"}{16}$, it follows from equation (3-3) that

$$F_i = \frac{60}{0.48\left(\frac{5}{16}\right)} \quad \text{or,}$$

$$F_i = 400 \quad \text{lb.}$$

For $x = 3\frac{1}{2}"$, $t = 0.1"$, $b = 10"$ and $2r = \frac{3"}{8}$, equation (2-41) gives

$$\sigma_\varepsilon = \frac{3 \times 60 \times 3.5}{2 \times 0.48 \times \frac{5}{16}\left(10 - \frac{3}{8}\right)(0.1)^2}$$

$$\sigma_\varepsilon = 21{,}818 \quad \text{psi.}$$

3.6 Stress Distribution in the Sign Face when an External Load Applied

The objective of this section is to determine the distribution of stresses along the x axis near hole B, for the sign face as shown in Figure 17. The experimentation is conducted after the bolts have been tightened by applying an external load and by measuring the surface strains in the y direction along the x axis near hole B. The strain gages are bonded directly to the surface of the sign face as in Section 3.2. Also, the same gage type and the same reading instruments were employed.

The experimental results are presented in Tables 7 and 8. The average stresses as determined experimentally are

compared, in this section, to the stresses computed using the equations presented in the last chapter. The comparison is made at corresponding points under identical loading conditions.

TABLE 7

SURFACE STRAINS IN THE SIGN FACE WHEN AN EXTERNAL TENSILE LOAD HAS BEEN APPLIED[a]

EXTERNAL LOAD F_e (lb)	TIGHTENING TORQUE (lb-in.)	STRAINS #1 (μin/in)	#2 (μin/in)	#3 (μin/in)	#4 (μin/in)
200	60	2635	1482	1114	936
	80	4106	2032	1356	1080
	100	4826	3748	2065	1419
400	60	2790	1898	1600	1414
	80	3910	2248	1752	1506
	100	4690	3883	2368	1803
600	60	3054	2329	2025	1844
	80	3992	2604	2145	1890
	100	4542	4009	2669	2156

[a]All the strains are compressive strain.

TABLE 8

SURFACE STRAINS IN THE SIGN FACE WHEN AN EXTERNAL COMPRESSIVE LOAD HAS BEEN APPLIED[b]

EXTERNAL LOAD F_e (lb)	TIGHTENING TORQUE (lb-in.)	STRAINS #1 (μin/in)	#2 (μin/in)	#3 (μin/in)	#4 (μin/in)
200	60	-3087	-1075	-336	-67
	80	-4514	-1684	-610	-200
	100	-5043	-3305	-1349	-529
400	60	-3212	-894	44	362
	80	-4610	-1506	-249	164
	100	-5125	-3145	-1038	-188
600	60	-3299	-716	366	730
	80	-4674	-1316	12	518
	100	-5187	-3006	-769	148

[b]A minus sign here indicates a compressive strain.

The corresponding stresses of the surface strains from Tables 7 and 8 were calculated by employing the stress-strain relationship presented in Section 3.2, and the results are tabulated in Tables 9 and 10 respectively.

When the distribution of stresses is plotted as a function of position along the x axis, the average stress can be obtained by using the same method outlined in Section 3.2. The first consideration deals with the distribution of stresses from Table 9. The average stress for a tightening torque of 60 lb-in. and an external tensile load of 200 lb from Figure 24,

is equal to 14,349 psi. Also, the average stress when the tightening torque is 60 lb-in. and the external tensile load is 400 lb from Figure 24, is equal to 18,429 psi.

The following example problems are presented to show the comparison between the average stress as determined experimentally and, the average stress computed by using either equation (2-47) or (2-48), under identical loading condition. In order to decide on which one of the two equations to use, it is necessary to compute the limiting value of F_e from

TABLE 9

SURFACE STRESSES IN THE SIGN FACE WHEN AN EXTERNAL TENSILE LOAD HAS BEEN APPLIED[c]

EXTERNAL LOAD F_e (lb)	TIGHTENING TORQUE (lb-in.)	STRESSES #1 (psi)	#2 (psi)	#3 (psi)	#4 (psi)
200	60	26350	14820	11140	9360
	80	41060	20320	13560	10800
	100	48260	37480	20650	14190
400	60	27900	18980	16000	14140
	80	39100	22480	17520	15060
	100	46900	38830	23680	18030
600	60	30540	23290	20250	18440
	80	39920	26040	21450	18900
	100	45420	40090	26690	21560

[c]All the stresses are compressive stress.

TABLE 10

SURFACE STRESSES IN THE SIGN FACE WHEN AN EXTERNAL COMPRESSIVE LOAD HAS BEEN APPLIED[d]

EXTERNAL LOAD F_e (lb)	TIGHTENING TORQUE (lb-in.)	STRESSES #1 (psi)	#2 (psi)	#3 (psi)	#4 (psi)
200	60	-30870	-10750	-3360	-670
	80	-45140	-16840	-6100	-2000
	100	-50430	-33050	-13490	-5920
400	60	-32120	-8940	440	3620
	80	-46100	-15060	-2940	1640
	100	-51250	-31450	-10380	-1880
600	60	-32990	-7160	3660	7300
	80	-46740	-13160	120	5180
	100	-51870	-30060	-7690	1480

[d]A minus sign here indicates a compressive stress.

equation (2-25); i.e.,

If $F_e < (F_e)_{limit}$, the average stress will be obtained by using equation (2-47).

If $F_e \geqslant (F_e)_{limit}$, the average stress will be obtained by using equation (2-48).

Example 1

When the bolt has been tightened to 60 lb-in. and an external tensile load of 200 lb had been applied, the limiting value of F_e from equation (2-25) can be expressed as:

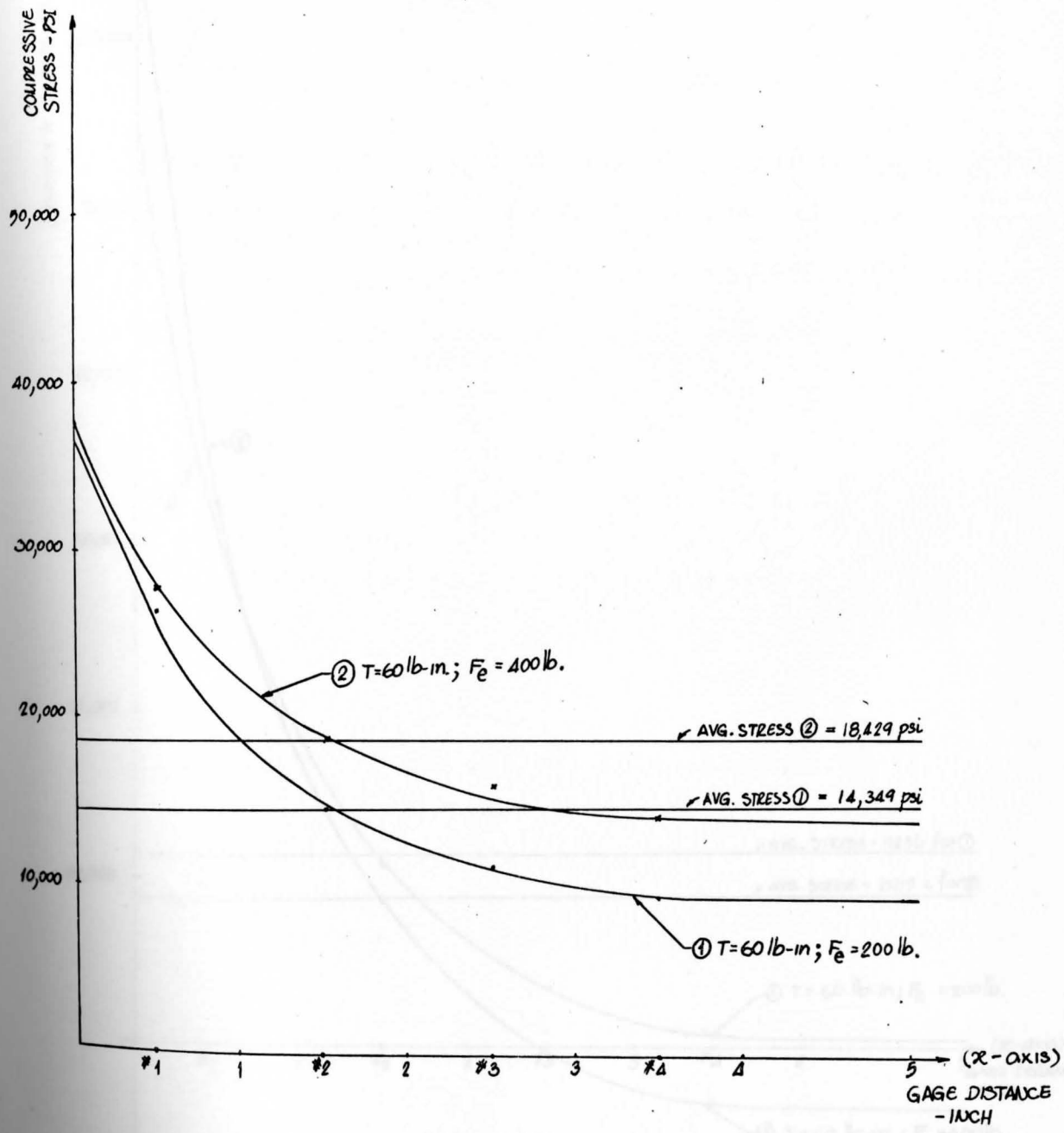

Figure 24 Distribution of Stresses along the x Axis, when an External Tensile Load has been applied.

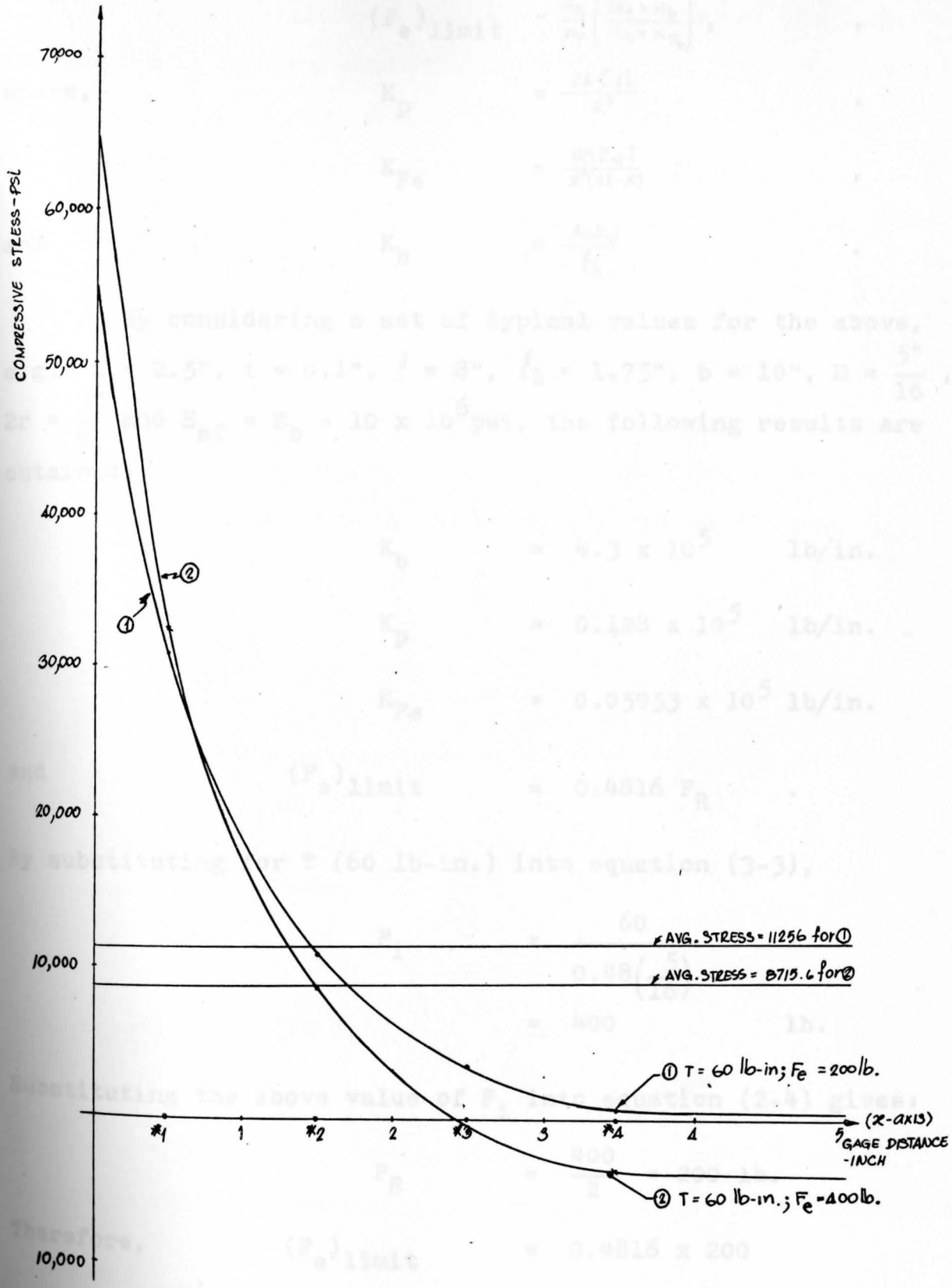

Figure 25 Distribution of Stresses along the x Axis, when an External Compressive Load has been applied

$$(F_e)_{limit} = \frac{K_{Fe}}{K_p}\left(\frac{2K_p + K_b}{K_b + K_{Fe}}\right)F_R \quad ,$$

where,

$$K_p = \frac{24\,E_{sf}I}{x^3} \quad ,$$

$$K_{Fe} = \frac{96\,E_{sf}I}{x^2(3l - x)} \quad ,$$

and

$$K_b = \frac{A_b E_b}{l_b} \quad .$$

By considering a set of typical values for the above, e.g., x = 2.5", t = 0.1", l = 8", l_b = 1.75", b = 10", D = $\frac{5"}{16}$, 2r = $\frac{3"}{8}$ and $E_{sf} = E_b = 10 \times 10^6$ psi, the following results are obtained:

$$K_b = 4.3 \times 10^5 \quad \text{lb/in.}$$

$$K_p = 0.128 \times 10^5 \quad \text{lb/in.}$$

$$K_{Fe} = 0.05953 \times 10^5 \quad \text{lb/in.}$$

and

$$(F_e)_{limit} = 0.4816\,F_R \quad .$$

By substituting for T (60 lb-in.) into equation (3-3),

$$F_i = \frac{60}{0.48\left(\frac{5}{16}\right)}$$

$$= 400 \quad \text{lb.}$$

Substituting the above value of F_i into equation (2-4) gives:

$$F_R = \frac{400}{2} = 200 \text{ lb.}$$

Therefore,

$$(F_e)_{limit} = 0.4816 \times 200$$

$$= 96.32 \quad \text{lb.}$$

The external load applied for a given test has been assumed to be uniform over the entire length (24") of the sign face. Since the force acting through a bolt includes only the force acting in the segment of the sign in the immediate vicinity of the bolt, it is necessary to find the proportion of the external load acting on a given segment. This can be done by partitioning the sign into segments of 7", 10" and 7" respectively from end to end and approximating the load on a given segment by its length to total length ratio. Following this procedure, the external load F_e on the central segment for a total load of 200 lb can be determined as follows:

$$F_e \simeq \frac{10}{24} \times 200 \simeq 83.3 \quad \text{lb}.$$

It results that: $F_e < (F_e)_{limit}$.

The average stress can be obtained by using equation (2-47), which follows:

$$\sigma_E = \frac{6}{(b-2r)t^2}\left[\frac{F_e l}{4} + \left(F_R - 2.0576F_e\right)\frac{\alpha}{2}\right] ,$$

$$\sigma_E = 62.33\left(1.25F_R - 0.572F_e\right) .$$

Now, substituting for F_R and F_e gives

$$\sigma_E = 12611.56 \quad \text{psi}.$$

Comparing the average stress as determined experimentally and the computed theoretical stress leads to a 12.1% difference.

Example 2

The bolt has been tightened to 60 lb-in. and an external tensile load of 400 lb is applied.

By calculation of $(F_e)_{limit}$ from equation (2-25), this example gives the same limiting value of F_e as in example 1. Since the same typical values have been substituted into equation (2-25), the following result is obtained:

$$(F_e)_{limit} = 97.20 \quad \text{lb.}$$

Following the procedure outlined previously, the portion of the total external load of 400 lb acting on the central 10" section is:

$$F_e \simeq \frac{400}{24} \times 10$$

$$\simeq 166.67 \quad \text{lb.}$$

It follows that: $F_e > (F_e)_{limit}$.

Therefore, the average stress can be obtained by using equation (2-48) as follows:

$$\Delta_E = \frac{F_e \ell}{4} \cdot \frac{6}{(b-2r)t^2} ,$$

$$= 166.67 \times 2 \times 62.33$$

$$= 20777.08 \quad \text{psi.}$$

Comparing the average stress as determined experimentally and the computed theoretical stress leads to an 11.3% difference.

The second consideration deals with the distribution of stresses from Table 10. The average stress for a tightening torque of 60 lb-in. and an external compressive load of 200 lb from Figure 25, is equal to 11,256 psi. Also, the average stress for a tightening torque of 60 lb-in. and an external compressive

load of 400 lb from Figure 25, is equal to 8,715.76 psi.

The following example problems are included to show the computation of the average stress by using equations (2-53) and (2-72), and to compare the computed results with those obtained experimentally, under identical loading condition.

Example 3

The bolt has been tightened to 60 lb-in. and an external compressive load of 200 lb has been applied. The average stress using equation (2-53) is computed in the first part of this example. The following results are obtained:

$$\sigma_E = \left[-\frac{F_e \ell}{4} + \left\{ \frac{K_p}{K_{Fe}} \left(\frac{K_b + K_{Fe}}{K_b + 2K_p} \right) F_e + F_R \right\} \frac{x}{\ell} \right] \frac{C}{I_E} \quad ,$$

where,

$$K_p = \frac{24 E_{sf} I}{x^3} \quad ,$$

$$K_{Fe} = \frac{96 E_{sf} I}{x^2 (3\ell - x)} \quad ,$$

and

$$K_b = \frac{A_b E_b}{\ell_b} \quad .$$

By substituting typical values of x = 3.0", t = 0.1", ℓ = 8", ℓ_b = 1.75", b = 10", 2r = $\frac{3}{8}$", $E_{sf} = E_b = 10 \times 10^6$ psi and ν_{Al} = 0.33, it follows that:

$$K_p = 0.0740 \times 10^5 \quad \text{lb/in.}$$

$$K_{Fe} = 0.04233 \times 10^5 \quad \text{lb/in.}$$

$$K_b = 4.3 \times 10^3 \quad \text{lb/in.}$$

Therefore,

$$\sigma_E = \frac{6}{(b-2r)t^2} \left[-\frac{F_e \ell}{4} + \left(1.7066 F_e + F_R \right) \frac{x}{\ell} \right] \quad ,$$

$$\sigma_E = 62.33\left(-2F_e + 2.5599F_e + 1.5F_R\right) ,$$

$$\sigma_E = 62.33\left(0.5599F_e + 1.5F_R\right) \quad . (3\text{-}4)$$

By substituting for T (60 lb-in.) into equation (3-3) gives

$$F_i = \frac{60}{0.48\left(\frac{5}{16}\right)}$$

$$= 400 \quad \text{lb.}$$

Substituting the above value of F_i into equation (2-4) gives

$$F_R = \frac{400}{2} = 200 \quad \text{lb.}$$

Following the procedure outlined previously, the portion of the total external load of 200 lb acting on the central 10" section is:

$$F_e \simeq 83.3 \quad \text{lb.}$$

By substituting for F_R and F_e into equation (3-4), the following result is obtained:

$$\sigma_E = 21607.39 \quad \text{psi.}$$

Comparing the average stress as determined experimentally and the computed theoretical stress leads to 48% difference.

The average stress is next computed by using equation (2-72). The following results are obtained:

$$\sigma_E = \left[-\frac{F_e l}{4} + \left\{\frac{K_{plate}}{K_{Fe}}\left(\frac{K_b + K_{Fe}}{K_b + K_{plate}}\right)\frac{F_e}{2} + F_R\right\}\frac{x}{2}\right]\frac{C}{I_E} ,$$

where,

$$K_{plate} = \frac{m^2 E t^3 (1 + 0.462\alpha^4)}{0.203\, x^2 (m^2 - 1)} ,$$

$$K_{Fe} = \frac{96 E_s I}{x^2(3l-x)} ,$$

$$K_b = \frac{A_b E_b}{l_b} .$$

Using the same typical values as in the first part, it follows that:

$$K_{plate} = 0.06165 \times 10^5 \quad \text{lb/in.}$$

$$K_{Fe} = 0.04233 \times 10^5 \quad \text{lb/in.}$$

$$K_b = 4.3 \times 10^5 \quad \text{lb/in.}$$

Since $F_e \simeq 83.33$ lb and $F_R = 200$ lb as in the first part,

$$\Delta_E = 62.33 \, (-2F_e + 1.08752F_e + 1.5F_R) ,$$

$$\Delta_E = 62.33 \, (-.9125F_e + 1.5F_R) ,$$

$$\Delta_E = 13959.6 \quad \text{psi.}$$

Comparing the average stress as determined experimentally and the computed theoretical stress leads to a 19.3% difference.

Example 4

The bolt has been tightened to 60 lb-in. and an external compressive load of 400 lb has been applied. The first part of this example will show the computation of the average stress by using equation (2-53) as in example 3. Using the same typical values as before,

$$\Delta_E = 62.33 \, (0.55996F_e + 1.5F_R) . \quad (3\text{-}5)$$

Using equations (3-3) and (2-4) yields

$$F_R = 200 \quad \text{lb.}$$

Following the procedure outlined previously, the portion of the total external load of 400 lb acting on the central 10" section is:

$$F_e \approx 166.66 \quad \text{lb.}$$

By substituting the above values for F_R and F_e into equation (3-5) gives:

$$\sigma_E = 24515.8 \quad \text{psi.}$$

Comparing the average stress as determined experimentally and the computed theoretical stress leads to a 64.4% difference.

Now, the average stress σ_E is computed by using equation (2-72). Following the method of example 3,

$$\sigma_E = 62.33\ (-.9125F_e + 1.5F_R) \quad .$$

By substituting for $F_e \simeq 166.66$ lb and $F_R = 200$ lb, leads to:

$$\sigma_E = 9220 \quad \text{psi.}$$

Comparing the average stress as determined experimentally and the computed theoretical stress leads to a 5.5% difference.

3.7 Bolt Strain Readings with an External Load Applied to the Post-Face Connection

The same "Strainsert" bolt and instruments described in Section 3.3 were employed here. This part of the experimentation was included in order to determine the tensile force in the bolt

when an external load has been applied. It was necessary to use the calibrated bolt strain readings VS tensile load relationship as obtained previously from the curve in Figure 22.

The experimental results for this section are presented in Tables 11 and 12. The tensile stress in the bolt as determined experimentally was compared to the tensile stress calculated from the equations derived in the previous chapter (2-55), (2-56), (2-58) and (2-71).

Also included in this part are experimental bolt strain readings for different hole locations, A, B, and C respectively. The experimental results in which the distribution of the applied external load can be determined by calculating the percentage of strain (or stress) for each bolt is tabulated in Tables 13 and 14.

The following example will show how the tensile force in the bolt, as tabulated in Tables 11 and 12, was obtained from the bolt strain reading.

For Tables 11 and 12, the bolt strain readings were obtained by conducting the experiment with the bolt at hole C. For a tightening torque of 10 lb-in. and an external tensile load of 200 lb, the strain reading was 1425 as tabulated in Table 11.

Thus, the tensile force in the bolt can be computed as follows:

$$\text{Tensile force} = \frac{1425}{19.111} = 74.56 \text{ lb.}$$

TABLE 11

BOLT STRAIN READINGS AT HOLE C, WITH A TENSILE-TYPE EXTERNAL LOAD APPLIED

TIGHTENING TORQUE (lb-in.)	EXTERNAL LOAD F_e (lb)	STRAIN READINGS	TENSILE FORCE (lb)
10	0	1300	68.02
	200	1425	74.56
	400	1864	97.54
	600	2694	140.97
20	0	2582	135.10
	200	2452	128.30
	400	2842	148.71
	600	3526	184.50
30	0	3964	207.42
	200	3168	165.77
	400	3310	173.20
	600	3894	203.76
40	0	6787	355.14
	200	5645	295.38
	400	5227	273.51
	600	5588	292.40

TABLE 12

BOLT STRAIN READINGS AT HOLE C, WITH A COMPRESSIVE EXTERNAL LOAD APPLIED

TIGHTENING TORQUE (lb-in.)	EXTERNAL LOAD F_e (lb)	STRAIN READINGS	TENSILE FORCE (lb)
10	0	1297	67.87
	200	1324	70.22
	400	2054	107.48
	600	2620	137.09
20	0	2546	133.22
	200	3264	170.79
	400	4152	217.25
	600	5179	270.99
30	0	4081	213.54
	200	5084	266.02
	400	6185	323.64
	600	6954	363.87
40	0	6653	348.12
	200	7784	407.30
	400	8807	460.83
	600	9819	513.79

TABLE 13

BOLT STRAIN READINGS AT HOLES A, B, AND C WITH A TENSILE-TYPE EXTERNAL LOAD APPLIED

TIGHTENING TORQUE (lb-in.)	EXTERNAL LOAD (lb)	STRAIN READINGS AT HOLE A	STRAIN READINGS AT HOLE B	STRAIN READINGS AT HOLE C	PORTION(%) OF F_e ACTING ON SECTION C
10	0	1814	1586	1008	0
	200	2314	2324	1210	20.6
	400	3268	3900	1978	21.62
	600	4362	5562	2882	22.5
20	0	4664	4686	3530	0
	200	3628	3802	3568	32.44
	400	3676	4212	3719	32.0
	600	4425	5500	3966	28.5
30	0	7084	8012	6344	0
	200	5980	7966	5412	27.96
	400	5076	6148	5552	33.1
	600	5046	6488	5730	33.19

The portion (by percent) of the total external load, acting on the section of the post-face which consists of hole C, can be determined as follows:

From the experimental data in Table 13, for a torque of 10 lb-in. and, an external load of 200 lb, it follows that:

the bolt strain reading at hole A = 2314

TABLE 14

BOLT STRAIN READINGS AT HOLES A, B, AND C WITH A COMPRESSIVE EXTERNAL LOAD APPLIED

TIGHTENING TORQUE (lb-in.)	EXTERNAL LOAD F_e (lb)	STRAIN READINGS AT HOLE A	STRAIN READINGS AT HOLE B	STRAIN READINGS AT HOLE C	PORTION(%) OF F_e ACTING ON SECTION C
10	0	1968	1754	1246	0
	200	2764	2500	1282	19.6
	400	3926	3554	1712	18.62
	600	4956	4528	2560	21.26
20	0	3936	4364	2624	0
	200	5098	5444	2945	21.84
	400	6196	6524	3900	23.46
	600	7186	7518	4832	24.75
30	0	6488	7170	5385	0
	200	7832	8190	6278	28.15
	400	8855	9274	7240	28.54
	600	9840	9980	8254	29.4

the bolt strain reading at hole B = 2324

the bolt strain reading at hole C = 1210

Therefore, the portion of the total load at hole C can be calculated as:

$$\% \text{ Load at hole C} = \frac{1210}{(2314 + 2324 + 1210)} \times 100 \ ,$$

$$= 20.6\% \quad .$$

In other words, the load applied to the section that contains hole C is equal to 20.6 percent of total external load of 200 lb, or 41.2 lb.

The following example problems are presented to show the comparison between the experimental results of the bolt stress presented in this chapter and, the theoretical bolt stress using the equations derived in the last chapter.

Example 1

Given a tightening torque of 10 lb-in. and an external tensile-type load of 400 lb. The tensile stress in the bolt can be computed by using either equation (2-55) or (2-56). In order to make a decision on which equation to use, it is necessary to compute the limiting value of F_e from equation (2-25); i.e.,

$$(F_e)_{limit} = \frac{K_{Fe}}{K_p}\left(\frac{K_b + 2K_p}{K_b + K_{Fe}}\right) F_R \quad ,$$

where,

$$K_p = \frac{24 E_{sf} I}{x^3} \quad ,$$

$$K_{Fe} = \frac{96 E_{sf} I}{x^2(3\ell - x)} \quad ,$$

and

$$K_b = \frac{A_b E_b}{\ell_b} \quad .$$

By substituting the typical values of x = 2.5", ℓ = 8", ℓ_b = 1.75", b = 8", t = 0.1", D = $\frac{5"}{16}$, 2r = $\frac{3"}{8}$, and $E_{sf} = E_b = 10 \times 10^6$ psi, the following results are obtained:

$$K_p = 0.1024 \times 10^5 \quad \text{lb/in.}$$

$$K_{Fe} = 0.0476 \times 10^5 \quad \text{lb/in.}$$

$$K_b = 4.3 \times 10^5 \quad \text{lb/in.}$$

and, $$(F_e)_{limit} = 0.4816 F_R \quad \text{lb.}$$

Substituting for T (10 lb-in.) into equation (3-3) gives

$$F_i = \frac{10}{0.48\left(\frac{5}{16}\right)} \quad ,$$

$$F_i = 66.66 \quad \text{lb.}$$

Substituting the above value of F_i into equation (2-4) yields

$$F_R = \frac{66.66}{2} = 33.33 \quad \text{lb.}$$

Therefore, $(F_e)_{limit} = 16.05$ lb.

From Table 13, the portion of the total external load on this section is 21.62 percent.

That is, $$F_e = \frac{21.62 \times 400}{100}$$

$$= 86.5 \quad \text{lb.}$$

It follows that: $F_e > (F_e)_{limit}$

Hence, the tensile stress will be obtained by using equation (2-55), or,

$$\sigma_b = \frac{F_e}{A_b} \quad ,$$

$$\sigma_b = \frac{86.48}{0.0767} \quad ,$$

$$\sigma_b = 1127.5 \quad \text{psi.}$$

From the experimental results, Table 11, the tensile force in the bolt for this case is 97.5 lb. The tensile stress in the bolt, dividing by it's area, is:

$$\sigma_b = \frac{97.5}{0.0767} = 1271.7 \quad \text{psi.}$$

Comparing the above two values of the tensile bolt stress leads to an 11.3% difference.

Example 2

Given a tightening torque of 10 lb-in. and an external compressive load of 400 lb. The tensile stress is obtained by using equations (2-58) and (2-71).

First, the tensile stress, σ_b, is determined by using equation (2-58), i.e.,

$$\sigma_b = \frac{\left[2\frac{K_p}{K_{Fe}}\left(\frac{K_b+K_{Fe}}{K_b+2K_p}\right)-1\right]F_e + 2F_i}{A_b} .$$

By substituting the typical values of $x = 3\frac{1}{4}$", $\ell = 8$", $\ell_b = 1\frac{3}{4}$", $b = 8$", $t = 0.1$", $D = \frac{5}{16}$", $2r = \frac{3}{8}$" and $E_{sf} = E_b = 10 \times 10^6$ psi. The following results are obtained:

$$K_p = 0.0466 \times 10^5 \quad \text{lb/in.}$$

$$K_{Fe} = 0.0292 \times 10^5 \quad \text{lb/in.}$$

$$K_b = 4.3 \times 10^5 \quad \text{lb/in.}$$

From Table 14, the proportion of the total load acting on this segment is equal to 18.62 percent.

That is $F_e = \frac{18.62 \times 400}{100}$,

$$F_e = 74.5 \quad \text{lb.}$$

For the tightening torque of 10 lb-in., and using equations (3-3) and (2-4) gives

$$F_R = 33.33 \quad \text{lb.}$$

It follows that: $\sigma_b = \frac{226.4}{0.0767} = 2952.3 \quad \text{psi.}$

Now, using equation (2-71) to determine the tensile stress,

$$\sigma_b = \frac{\left[\frac{K_{plate}}{K_{Fe}}\left(\frac{K_b + K_{Fe}}{K_b + K_{plate}}\right) - 1\right] F_e + 2F_R}{A_b} ,$$

where, $K_{plate} = \frac{m^2 E t^3 (1 + 0.462\alpha^4)}{0.203\, x^2 (m^2 - 1)}$.

By substituting the same typical values as before, the following results are obtained:

$K_{plate} = 0.05299 \times 10^5$ lb/in.

$K_{Fe} = 0.0292 \times 10^5$ lb/in.

$K_b = 4.3 \times 10^5$ lb/in.

Since, $F_e = 74.5$ lb,

and $F_R = 33.33$ lb,

$\sigma_b = \frac{126.62}{0.0767} = 1650.8$ psi.

From the experimental results, Table 12, the tensile force in the bolt in this case is equal to 107.5 lb. Dividing this by the bolts' area gives an experimental bolt-stress of

$$\sigma_b = \frac{107.5}{0.0767} = 1401.3 \quad \text{psi.}$$

Comparing the tensile bolt stress from the above experimental result and from equation (2-58) leads to 52.2% difference.

Comparing the tensile bolt stress from the above experimental result and from equation (2-71) leads to 15.1% difference.

Example 3

Given a tightening torque of 20 lb-in., and an external tensile-type load of 600 lb. The tensile stress in the bolt can be computed by using either equation (2-55) or (2-56). A limiting value of F_e can be obtained as in example 1 and, using the same typical values as before in (2-25), gives the following result:

$$(F_e)_{limit} = 0.4816 F_R \quad \text{lb.}$$

Substituting for T (20 lb-in.) into equation (3-3) gives

$$F_i = \frac{20}{0.48\left(\frac{5}{16}\right)}$$

$$F_i = 133.33 \quad \text{lb.}$$

Substituting the above value of F_i into equation (2-4) gives

$$F_R = \frac{133.33}{2} = 66.66 \quad \text{lb.}$$

Thus, $(F_e)_{limit} = 0.4816 \times 66.66$

$$(F_e)_{limit} = 32.1 \quad \text{lb.}$$

From Table 13, the proportion of the total external load acting on this segment is equal to 28.5 percent.

That is, $$F_e = \frac{28.5}{100} \times 600$$

$$= 171 \quad \text{lb.}$$

It then follows that: $F_e > (F_e)_{limit}$.

Dividing the above by the area, gives the tensile stress; i.e.,

$$\sigma_b = \frac{F_e}{A_b} \quad ,$$

$$\sigma_b = \frac{171}{0.0767} \quad ,$$

$$\sigma_b = 2229.5 \quad \text{psi.}$$

From the experimental results, Table 11, the tensile force in the bolt is equal to 184.5 lb which gives a tensile stress of:

$$\sigma_b = \frac{184.5}{0.0767} = 2405.5 \quad \text{psi.}$$

Comparing the above two values of tensile bolt stress leads to a 7.3% difference.

Example 4

Given a tightening torque of 20 lb-in. and an external compressive load of 600 lb. The tensile stress is obtained by using equations (2-58) and (2-71).

Repeating the procedure outlined in the last three examples by first substituting into equation (2-58) gives:

$$\sigma_b = \frac{(2.145)\, F_e + 2F_R}{A_b} \quad .$$

From Table 14, the proportion of the total external load acting on the segment is equal to 24.75 percent.

Then, $F_e = \frac{24.75 \times 600}{100} = 148.5$ lb,

and since $F_R = 66.66$ lb,

it follows that $\sigma_b = \frac{451.86}{0.0767} = 5891.3$ psi.

Now, using equation (2-71), and the same typical values as before leads to:

$$\sigma_b = \frac{0.804F_e + 2F_R}{A_b} \quad ,$$

and substituting $F_e = 148.5$ lb and $F_R = 66.66$ lb gives

$$\sigma_b = \frac{252.84}{0.0767} = 3296.5 \text{ psi.}$$

From the experimental results, Table ,2, the tensile force in the bolt is equal to 270.9 lb and the tensile stress will be:

$$\sigma_b = \frac{270.9}{0.0767} = 3533.1 \text{ psi.}$$

Comparing the tensile bolt stress from the above experimental result and from equation (2-58) leads to a 40% difference.

Comparing the tensile bolt stress from the above experimental result and from equation (2-71) leads to a 6.7% difference.

CHAPTER IV

EXPERIMENTAL FATIGUE INVESTIGATIONS

4.1 Introduction

From a previous investigations [1], it was found that it would not be practical to determine the fatigue properties of signs and their related hardware through the use of field mounted sign installations, because of the following obvious reasons:

1. the lack of control over atmospheric wind conditions and,
2. the long time period required to achieve a fatigue failure.

Therefore, it was decided, in both the referenced and current study, to determine the fatigue properties of the present and proposed sign systems by subjecting them to mechanical oscillatory-type tests. The MTS machine was selected for the conduct of these tests.

Thus, the purpose of this chapter is the establishment of the fatigue strength of the typical sign face fastened to a standard post with various initial bolt torques and connection modifications. Because of the size of the loading frame of the MTS machine, the sign blank material was reduced in size, as compared to a true sign,as shown in Figure 2. Therefore, the common size face used in the experimentation was 12" x 24" with

a span of 8". The 24" length dimension allows for a hole spacing of 10" center-to-center and a 2" center-to-edge dimension.

In order to minimize the testing time, the testing frequency was as high as possible and the dynamic load applied was selected so as to cause a stress, at the most critically stresses section, in excess of the fatigue strength of the face material. Therefore, a desirable dynamic load for this test would be 600 lb (see Appendix A).

4.2 Standard Connection

The sign face blank was fastened to a standard post and a bending-type load was applied directly to the arrangement as shown in Figure 26 below.

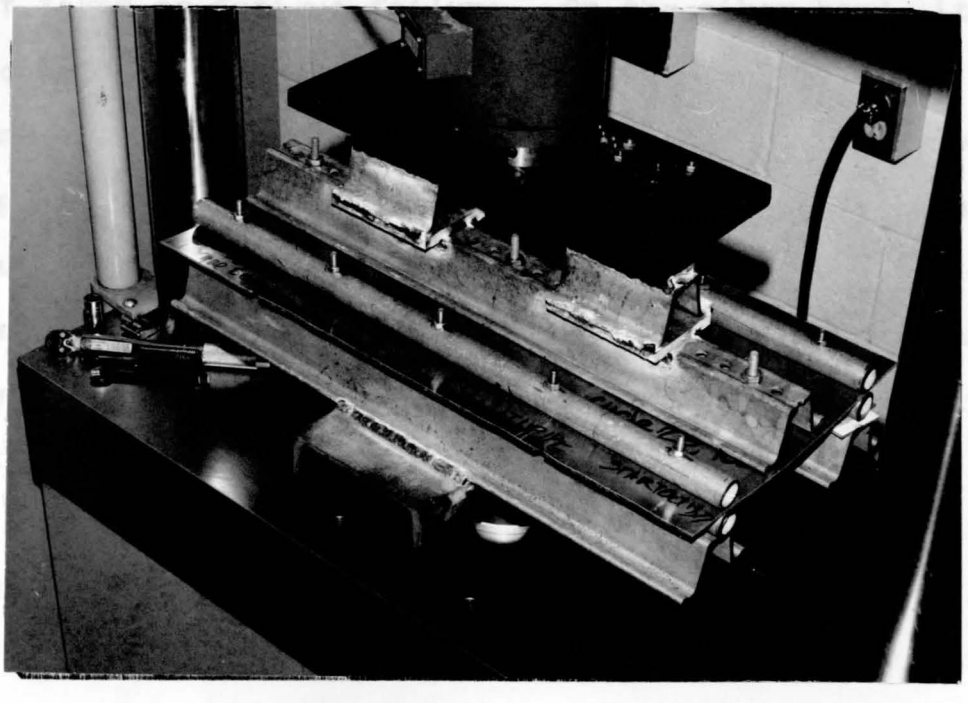

Figure 26 Photograph of Standard Connection

4.2.1 Testing Procedures and Results

In the conduct of these tests, an oscillating-type bending load with an amplitude of $\pm$ 600 lb was selected. The Servo Controller of the MTS was adjusted to produce the displacement amplitudes that resulted in the desired loading. The test frequency used was 1.2 hz. This resulted from the inability of the servo-system to respond to the required displacement amplitudes at higher frequencies. The results of the fatigue testing conducted using the standard $\frac{5"}{16}$ aluminum bolt and flat washer are given in Table 15.

The face in each test was inspected by the naked eye for cracks after approximately every ten to twenty thousand cycles. When the first crack appeared, it was so fine that it was hardly noticeable by the naked eye. Thus, this condition was not taken as fatigue failure. On the other hand, it was not necessary to continue a test to the point where the sign face was torn completely loose from the post in order to create a fatigue failure. Then, it follows that the establishment of a failure criteria was required. Therefore, it was decided to consider a fatigue failure as having occurred with a crack originating at the mounting hole and propagating radially outward to a length of $\frac{1"}{4}$.

In some tests, there were a number of cracks at the mounting hole that could not be seen by the naked eye. In order to complete the inspection in this case and determine the number of cracks and their length of propagation, it was necessary to use a dye penetrant which was capable of detecting

TABLE 15

TABULATION OF FATIGUE TESTS USING A STANDARD CONNECTION

TEST NUMBER	NOM. GAUGE THICKNESS	POST TYPE	BOLT TORQUE (lb-in.)	TEST FREQUENCY (CPS)	DYNAMIC LOAD (lb)	NUMBER OF CYCLES	FAILURE NOTES / CRACK LENGTHS IN INCHES
16 A							2R - $\frac{1"}{4}$ MAX.
B	0.1	NO. 4 STEEL	60	1.2	±600	178,687	1P - $1\frac{3"}{4}$
C							2R - $\frac{3"}{16}$ MAX; 1P - $1\frac{1}{2}$"
17 A							2R - $\frac{1"}{4}$ MAX.
B	0.1	"	60	1.2	±600	164,078	1P - $2\frac{1}{4}$"
C							NO CRACKS
18 A							2R-$\frac{1"}{4}$ MAX; 2P-3" MAX.
B	0.1	"	60	1.2	±600	238,553	2P - 2" MAX.
C							2R - $\frac{1"}{16}$ MAX; 1P - $1\frac{3"}{4}$

TABLE 15 CONTINUED

TEST NUMBER	NOM. GAUGE THICKNESS	POST TYPE	BOLT TORQUE (lb-in.)	TEST FREQUENCY (CPS)	DYNAMIC LOAD (lb)	NUMBER OF CYCLES	FAILURE NOTES CRACK LENGTHS IN INCHES
19 A							4R - $\frac{1"}{4}$ MAX.
B	0.1	NO. 4 STEEL	60	1.2	±600	167,200	1R - $\frac{1"}{16}$
C							NO CRACKS
5 A							1R - $\frac{1"}{4}$
B	0.1	"	80	1.2	±600	109,131	1P - $\frac{1"}{2}$
C							3R - $\frac{1"}{4}$ MAX; 1P - $1\frac{3"}{4}$
9 A							2R - $\frac{1"}{4}$ MAX; 1P - $1\frac{1}{2}"$
B	0.1	"	80	1.2	±600	106,620	NO CRACKS
C							1R - $\frac{1"}{4}$

TABLE 15 CONTINUED

TEST NUMBER	NOM. GAUGE THICKNESS	POST TYPE	BOLT TORQUE (lb-in.)	TEST FREQUENCY (CPS)	DYNAMIC LOAD (lb)	NUMBER OF CYCLES	FAILURE NOTES / CRACK LENGTHS IN INCHES
12 A							4R - $\frac{1}{4}$" MAX.
B	0.1	NO. 4 STEEL	80	1.2	±600	163,596	1P - $2\frac{1}{4}$"
C							1P - $2\frac{1}{8}$"
14 A							1R - $\frac{1}{4}$" MAX.
B	0.1	"	80	1.2	±600	150,940	1P - $1\frac{1}{2}$"
C							1R - $\frac{1}{8}$"; 1P - $\frac{3}{4}$"
6 A							3R - $\frac{1}{4}$" MAX.
B	0.1	"	100	1.2	±600	80,000	2R-$\frac{1}{4}$" MAX; 2P-1" MAX.
C							2R - $\frac{1}{4}$" MAX; 1P - $\frac{1}{2}$"

TABLE 15 CONTINUED

TEST NUMBER	NOM. GAUGE THICKNESS	POST TYPE	BOLT TORQUE (lb-in.)	TEST FREQUENCE (CPS)	DYNAMIC LOAD (lb)	NUMBER OF CYCLES	FAILURE NOTES / CRACK LENGTHS IN INCHES
10 A							2R - $\frac{1}{4}$" MAX.
B	0.1	NO. 4 STEEL	100	1.2	±600	100,402	NO CRACKS
C							1P - $1\frac{1}{4}$"
11 A							3R - $\frac{1}{4}$" MAX.
B	0.1	"	100	1.2	±600	81,000	NO CRACKS
C							2R - $\frac{1}{4}$" MAX; 1P - $1\frac{3}{4}$"
13 A							1R - $\frac{1}{4}$"
B	0.1	"	100	1.2	±600	101,000	NO CRACKS
C							1R - $\frac{1}{16}$"; 1P - $\frac{5}{8}$"

TABLE 15 CONTINUED

TEST NUMBER	NOM. GAUGE THICKNESS	POST TYPE	BOLT TORQUE (lb-in.)	TEST FREQUENCY (CPS)	DYNAMIC LOAD (lb)	NUMBER OF CYCLES	FAILURE NOTES / CRACK LENGTHS IN INCHES
7 A							1R - $\frac{3"}{16}$
B	0.1	NO. 4 STEEL	120	1.2	±600	76,200	2R - $\frac{3"}{16}$ MAX; 1P - $1\frac{1}{4}$"
C							2R - $\frac{1"}{4}$ MAX; 1P - 1"
8 A							2R - $\frac{1"}{4}$ MAX; 1P - $\frac{1"}{2}$
B	0.1	"	120	1.2	±600	77,400	1R - $\frac{1"}{8}$
C							2R - $\frac{1"}{16}$ MAX.
15 A							1P - $\frac{1"}{4}$
B	0.1	"	120	1.2	±600	98,000	1R - $\frac{1"}{4}$
C							1P - 2"

the finest of cracks.

Two types of cracks occurred in the tests; namely, a radial type, noted by R in Table 15, which originates at the mounting hole and propagates radially outward; and, a parallel-type, noted by P, which is parallel to the post along the line of contact between the post and sign face.

A close-up of the fatigue cracks for the standard connection is shown in Figure 27. From the results of the fatigue testing presented in Table 15, it is seen that excessive fastener bolt torque tends to greatly reduce the fatigue strength of a sign.

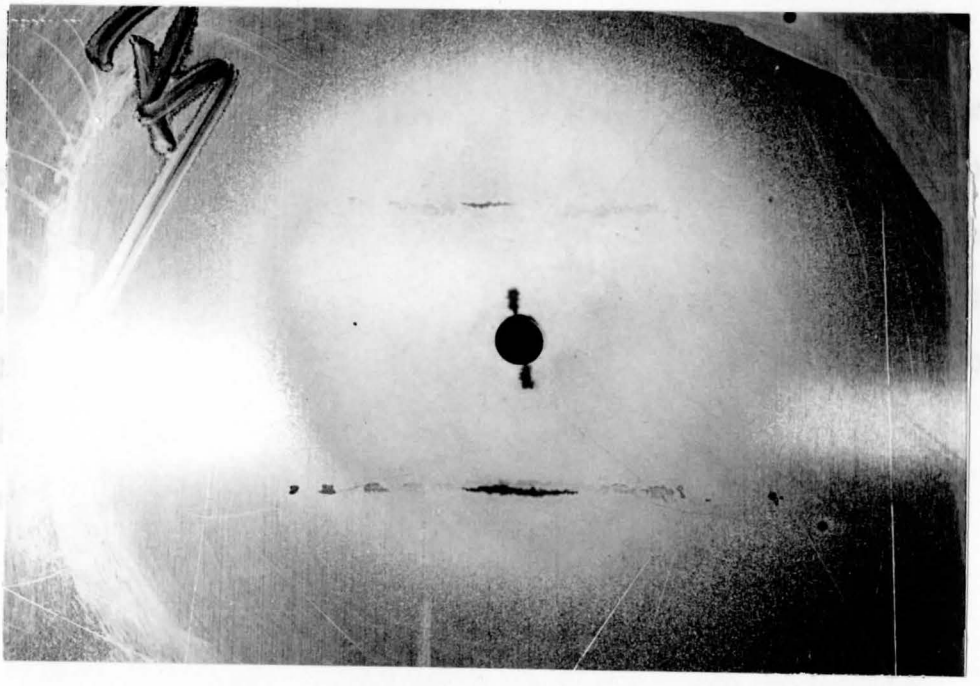

Figure 27 Photograph of Typical Cracks for Standard Connection

4.3 Modified Connection

In an effort to reduce or eliminate the parallel-type cracks obtained with the standard connection, the face blank was fastened to the post with half pipes mounted along the entire length of each edge of the post between the post and blank as shown in Figure 28. A steel pipe $1\frac{3}{8}$" outside diameter and 24" in length was cut into halves as shown in Figure 29.

4.3.1 Testing Procedures and Results

In this test, the same oscillating-type bending load, test frequency, and procedure were used as was used for the standard connection tests. The results of the fatigue testing conducted in this case are given in Table 16.

Inspecting the sign face for cracks, as was done previously, showed radial-type cracks at the mounting hole area. The parallel-type cracks which would be in line with the pipe were eliminated, that is, the bending stress along this line was reduced and transmitted to the mounting hole area. The fatigue failure criteria for this test was the same as used in the standard connection testing.

A close-up view of the fatigue cracks of a test using this modified connection is shown in Figure 30.

TABULATION OF FATIGUE TESTS USING A MODIFIED CONNECTION

TEST NUMBER	NOM. GAUGE THICKNESS	POST TYPE	BOLT TORQUE (lb-in.)	TEST FREQUENCY (CPS)	DYNAMIC LOAD (lb)	NUMBER OF CYCLES	FAILURE NOTES CRACK LENGTHS IN INCHES
20 A							2R - $\frac{1"}{4}$ MAX.
B	0.1	NO. 4 STEEL	80	1.2	±600	161,733	1R - $\frac{3"}{16}$
C							3R - $\frac{1"}{4}$ MAX.
21 A							2R - $\frac{1"}{4}$ MAX.
B	0.1	"	80	1.2	±600	169,000	1R - $\frac{1"}{8}$
C							2R - $\frac{3"}{16}$ MAX.
25 A							1R - $\frac{1"}{4}$ MAX.
B	0.1	"	80	1.2	±600	145,364	NO CRACKS
C							2R - $\frac{3"}{16}$

TABLE 16 CONTINUED

TEST NUMBER		NOM. GAUGE THICKNESS	POST TYPE	BOLT TORQUE (lb-in.)	TEST FREQUENCY (CPS)	DYNAMIC LOAD (lb)	NUMBER OF CYCLES	FAILURE NOTES CRACK LENGTHS IN INCHES
26	A							NO CRACKS
	B	0.1	NO. 4 STEEL	80	1.2	±600	154,483	3R - $\frac{1"}{4}$ MAX.
	C							3R - $\frac{1"}{4}$ MAX.
22	A							2R - $\frac{1"}{8}$ MAX.
	B	0.1	"	100	1.2	±600	120,000	NO CRACKS
	C							2R - $\frac{1"}{4}$ MAX.
23	A							2R - $\frac{1"}{4}$ MAX.
	B	0.1	"	100	1.2	±600	88,314	NO CRACKS
	C							2R - $\frac{1"}{4}$ MAX.

TABLE 16 CONTINUED

TEST NUMBER	NOM. GAUGE THICKNESS	POST TYPE	BOLT TORQUE (lb-in.)	TEST FREQUENCY (CPS)	DYNAMIC LOAD (lb)	NUMBER OF CYCLES	FAILURE NOTES CRACK LENGTHS IN INCHES
24 A							1R - $\frac{1"}{16}$
B	0.1	NO. 4 STEEL	100	1.2	±600	83,000	NO CRACKS
C							2R - $\frac{1"}{4}$ MAX.
27 A							1R - $\frac{1"}{8}$
B	0.1	"	100	1.2	±600	110,000	NO CRACKS
C							2R - $\frac{1"}{4}$ MAX.

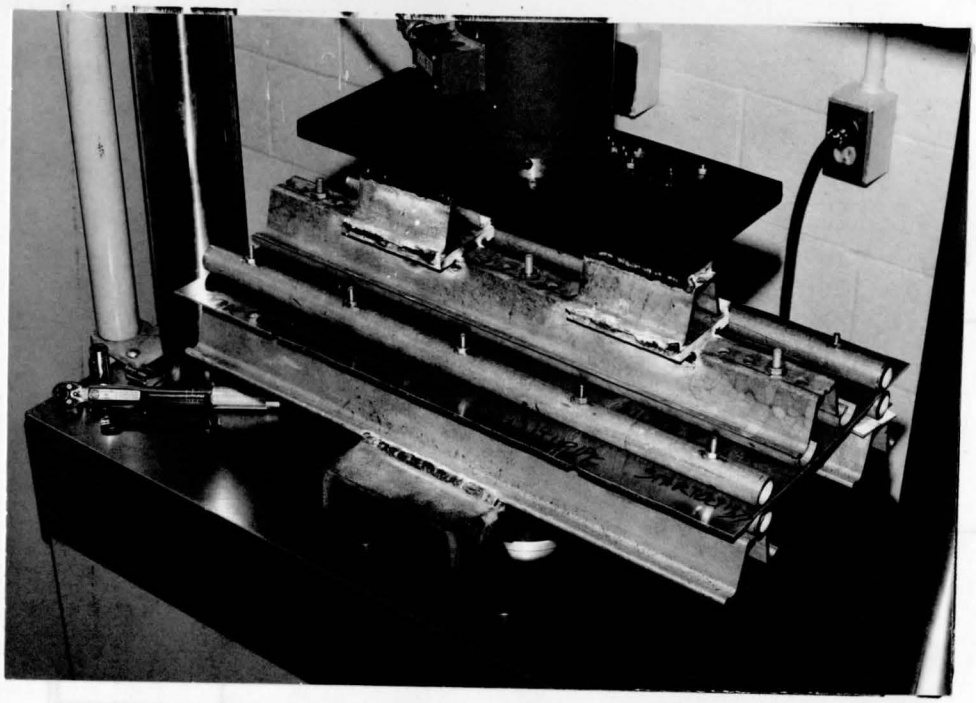

Figure 28 Photograph of Modified Connection

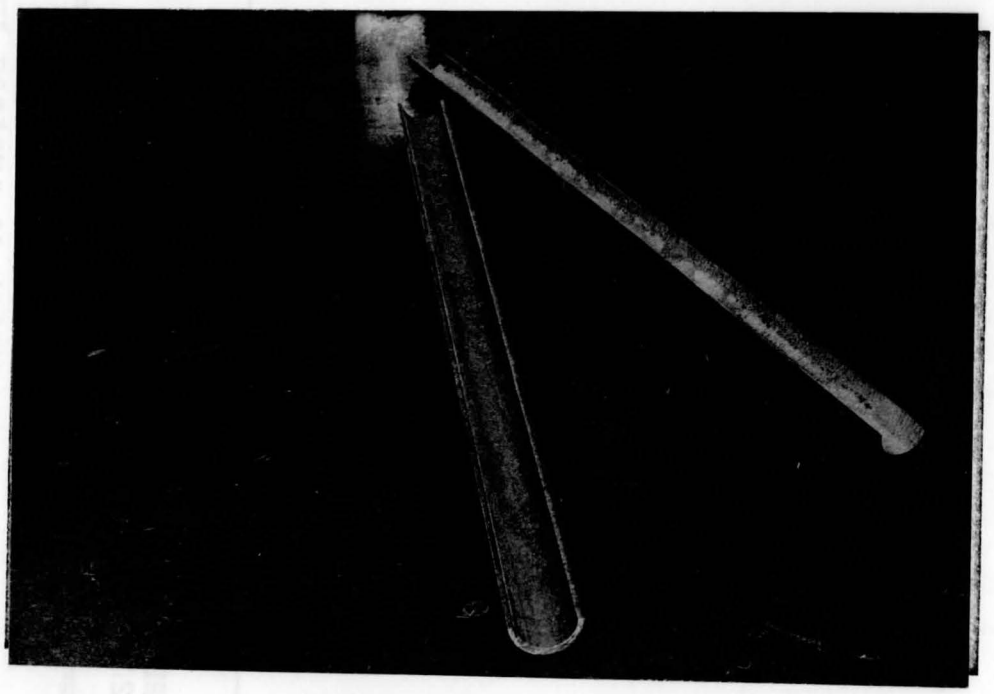

Figure 29 Photograph of Half Pipes

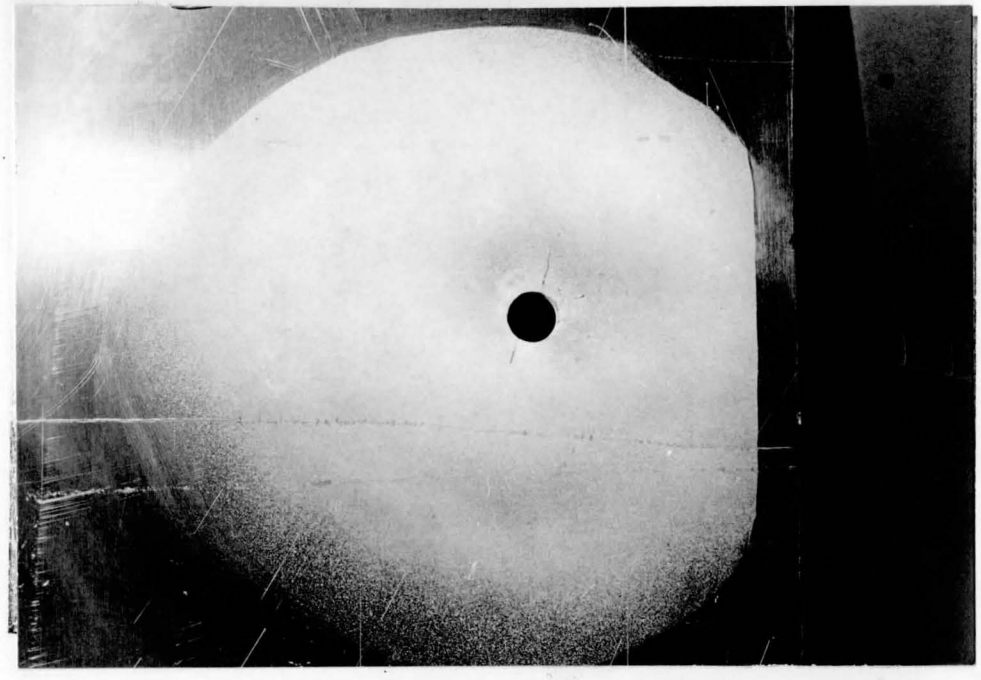

Figure 30 Photograph of Typical Cracks for Modified Connection

4.4 Connection with a Proposed Back-Up Plate

The sign face blank as fastened to a post when using the proposed back-up device under the direct loading arrangement is shown in Figure 31. The designed proposed back-up strip is shown in Figure 32. The strip consists simply of a strip of aluminum blanking material which has been deformed by bending over the edge of its mating post.

4.4.1 Testing Procedures and Results

The loading arrangement and frequency were the same as in the previous tests. The results of the fatigue testing for this case are given in Table 17:

TABLE 17

TABULATION OF FATIGUE TESTS USING A PROPOSED BACK-UP PLATE

TEST NUMBER	NOM. GAUGE THICKNESS	POST TYPE	BOLT TORQUE (lb-in.)	TEST FREQUENCY (CPS)	DYNAMIC LOAD (lb)	NUMBER OF CYCLES	FAILURE NOTES CRACK LENGTHS IN INCHES
28 A							2P - $1\frac{3}{4}$" MAX.
B	0.1	NO. 4 STEEL	80	1.2	±600	167,000	1P - $2\frac{1}{2}$"
C							NO CRACKS
29 A							2P - 2" MAX.
B	0.1	"	80	1.2	±600	171,924	1P - $2\frac{7}{8}$"
C							1P - 3"
30 A							1P - $2\frac{1}{8}$"
B	0.1	"	80	1.2	±600	140,000	1P - $1\frac{1}{2}$"
C							2P - 1" MAX.

TABLE 17 CONTINUED

TEST NUMBER	NOM. GAUGE THICKNESS	POST TYPE	BOLT TORQUE (lb-in.)	TEST FREQUENCY (CPS)	DYNAMIC LOAD (lb)	NUMBER OF CYCLES	FAILURE NOTES CRACK LENGTHS IN INCHES
33 A							1P - $1\frac{5}{8}$"
B	0.1	NO. 4 STEEL	80	1.2	±600	145,000	1P - $1\frac{3}{4}$"
C							2P - $1\frac{1}{2}$"
31 A							1P - $1\frac{1}{2}$"
B	0.1	"	100	1.2	±600	105,600	1P - $1\frac{7}{8}$"
C							2P - $1\frac{1}{4}$" MAX.
32 A							1P - $1\frac{1}{4}$"
B	0.1	"	100	1.2	±600	130,000	1P - $1\frac{3}{4}$"
C							2P - $1\frac{1}{4}$" MAX.

TABLE 17 CONTINUED

TEST NUMBER		NOM. GAUGE THICKNESS	POST TYPE	BOLT TORQUE (lb-in.)	TEST FREQUENCY (CPS)	DYNAMIC LOAD (lb)	NUMBER OF CYCLES	FAILURE NOTES CRACK LENGTHS IN INCHES
34	A							1P - $1\frac{1}{2}$"
	B	0.1	NO. 4 STEEL	100	1.2	±600	123,337	1P - $1\frac{1}{2}$"
	C							1P - $1\frac{3}{8}$"
35	A							1P - $1\frac{1}{2}$"
	B	0.1	"	100	1.2	±600	131,089	2P - 2" MAX.
	C							1P - $1\frac{3}{4}$"

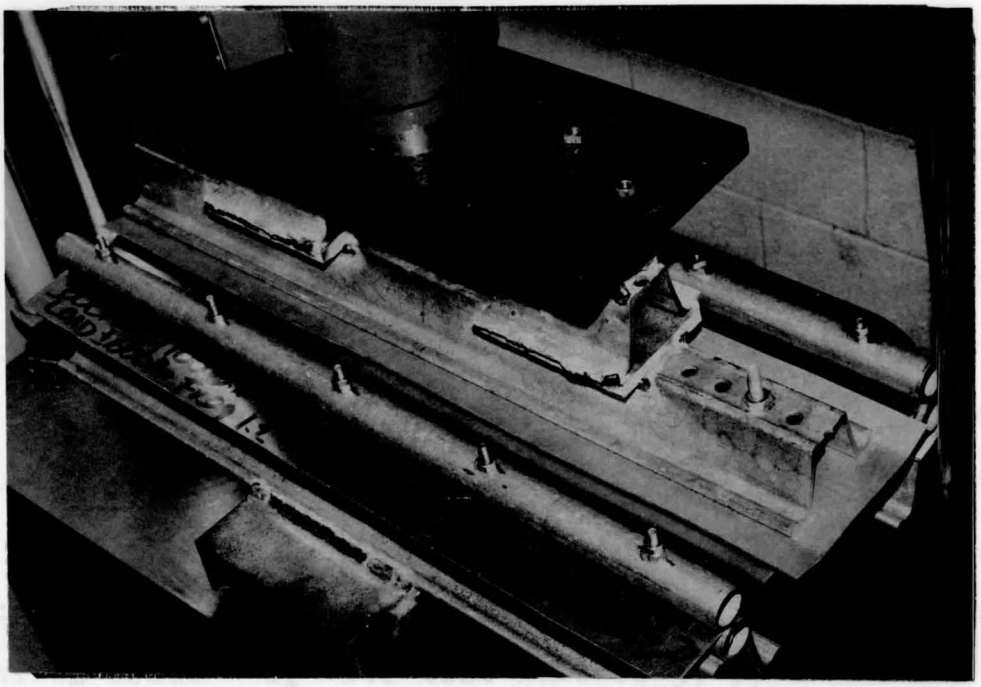

Figure 31 Photograph of Connection with a Proposed Back-Up Plate

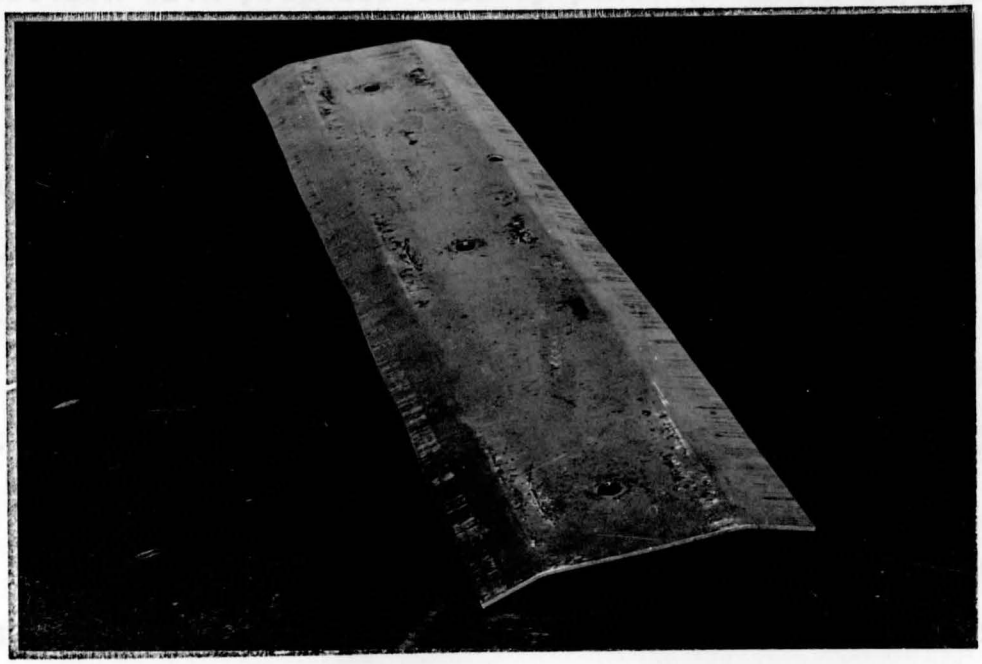

Figure 32 Photograph of Back-Up Strip

Inspection of the face for cracks with this test revealed the presence of the parallel-type cracks which were in line with the edge of the back-up plate. The radial-type cracks at the mounting hole were eliminated. This apparently results from the fact that the back-up plate carries some of the initial bending stress induced in the sign blank by the bolt.

In order to compare the results of this test with the results of the standard connection test, the failure criteria for this test was based on the maximum length of parallel-type crack from Table 15. For example, the maximum length of parallel crack = 2¼" for test numbers 5, 9, 12 and 14 (all at 80 lb-in. bolt torque). Therefore, the failure criteria was taken as a 2¼" long P-type crack for 80 lb-in. bolt-torque.

A close-up view of the fatigue cracks using the connection with proposed back-up plate is shown in Figure 33.

In conducting the tests for these three connections, the aluminum bolts were found to have adequate strength and managed to remain fastened. Also, the post involved never failed, and did not appear to have any detectable fatigue failure effects.

To assist in evaluating the fatigue test results contained in Tables 15, 16 and 17, the following notations and reference notes were used:

Each face has three holes and fasteners, denoted as A, B, C. A and C are the two outside holes, 2" away from their respective edges. Hole B is the center hole with a 10"

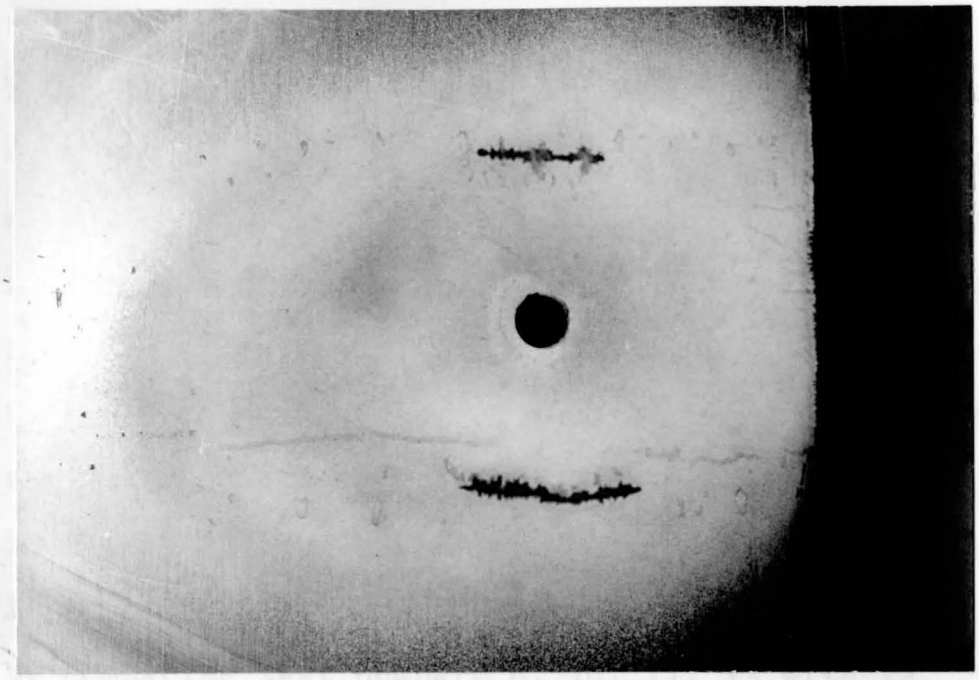

Figure 33 Photograph of Typical Cracks by Using Proposed Back-Up Plate

center-to-center dimension from A and C.

Bolt-torque refers to the initial torque applied to each of the fastening bolt nuts just prior to testing.

The fatigue cracks are referenced as "P" and "R", which designate parallel and radial cracks respectively as explained previously.

A close examination of the fatigue test results, tabulated in Tables 15, 16 and 17, reveals the following:

1. Excessive fastener bolt torque tends to greatly reduce the fatigue strength of a sign; e.g., compare test numbers 16, 17,18 and 19 (60 lb-in.) in which the number of cycles required to cause the cracks is significantly

greater than the number of cycles required for test numbers 7, 8 and 15.

2. There were some early failures in the standard connection when the same bolt torque and the same dynamic load were applied. This is evident from test numbers 5 and 9 which failed before test numbers 12 and 14 indicating some inconsistency of the results. This was not unexpected.
3. The use of the half steel pipe along the edge of the post was found to increase the fatigue strength of the system in comparison to the standard connection under the same loading condition and the same bolt torque. This appears by comparing test numbers 6, 10, 11, 13 with 22, 23, 24 and 27.
4. The use of the half steel pipe along the edge of the post eliminated the parallel type of cracking. However, the radial-type cracks continued to occur.
5. The use of the back-up device was found to improve the fatigue strength of a sign connection when compared to the standard connection. This follows by comparing test numbers 28, 29, 30, 33 with 5, 9, 12 and 14. It was also found that the use of the back-up plate resulted only in parallel-type cracks in line with the edge of the back-up.
6. In the modified connection and the connection with the proposed back-up plate, excessive fastener bolt torque also tends to reduce the fatigue strength of the system.

CHAPTER V

CONCLUSIONS AND DISCUSSION

5.1 Conclusions

In the analysis of the typical highway sign face to post connection, it was seen that simple beam theory can be applied when an external tensile-type load is applied to the post-face connection. In the case where an external compressive load was applied, the theoretical value of bolt force, equation (2-35), which was obtained by using simple beam theory, led to a poor correlation with experimental results. Therefore, it was decided to use plate theory for the deflection of the sign face under the bolt's load in this case in order to improve this correlation. The final formulations for bolt force, equation (2-70), was thus obtained.

The bending stress in the sign face at the mounting hole area, resulting from an initial preload, F_i, caused by tightening the bolts, can be determined by equation (2-41). The stresses at the mounting hole area resulting from the application of an external tensile load and compressive load can be determined by using equations (2-47) or (2-48) and (2-72), respectively. The fatigue loading in this project had the form of a sine wave which means that the applied load changes from a compressive amplitude in one direction to a tensile amplitude in the opposite direction. The fluctuating stress in the sign face at the

mounting hole area can then be determined based on the amplitude values. This is done in the next section.

The stress in the bolt resulting from:

1. the initial preload, F_i,
2. the application of an external tensile load, and
3. the application of a compressive load

can be determined by using equations (2-3), (2-55) or (2-56) and (2-71) respectively. Similarly, the fluctuating bolt stress can be determined and will be computed in the next section.

In conducting the static experimentation of the bolt and the sign face, as explained in Chapter III, the average stress at the mounting hole area resulting from an initial preload, F_i, (bolt torque), was obtained as described in Section 3.2 and the percentage difference of about 8 percent from the theoretical equation (2-41) was obtained. The average stress at the mounting hole area from the experimental results in Section 3.6, when an external load, F_e, was applied, produced a percentage difference of about 5 to 20 percent from the theoretical values given by equations (2-47), (2-48) and (2-72). In Section 3.7, the tensile stress in the bolt from the experimental results, when an external load, F_e, was applied, produced a difference of about 2 to 15 percent from the theoretical values given by equations (2-55), (2-56) and (2-71).

In the experimental fatigue investigations of the sign face to post connection using the MTS machine to subject current and proposed sign systems to stresses exceeding the fatigue limit,

the following can be concluded:

1. The most significant result was the effect of "over torqueing" of the fastener bolts. This greatly reduced the fatigue strength of the system.
2. The use of half steel pipes along the line of contact between the sign face and the edges of the post can improve the fatigue strength and reduce or eliminate the detrimental effect of localizing the load transmission, from face to post, along this line of contact.
3. The use of a back-up device can improve the fatigue strength and reduce or eliminate detrimental effect of localizing the load transmission at each mounting hole area.
4. The fastener bolts were found to have adequate strength and managed to remain fastened without any fatigue damage.

5.2 Discussion

When specific values were substituted into equations (2-53) and (2-72), derived using simple beam theory and plate theory respectively, and the analytical values compared to the experimental results at the same loading conditions, it was found that the analytical values obtained from beam theory lead to larger percentage differences than those resulting from plate theory. This was demonstrated through examples 3 and 4 in Section 3.6. Here it was shown that the average stress computed by using equation (2-53) led to a difference of about 48 percent from the experimental result. The average stress

computed by using equation (2-72) resulted in a difference of about 19 percent from the experimental value, in example 3 where plate theory was used.

In considering the mounting hole area, point E, the average stress at this point can be obtained by substituting specific values into equations (2-41), (2-47) or (2-48) and (2-72). Thus, the fluctuating bending stress in the sign face at the mounting hole area can be plotted as a function of time. For example, when the bolt was tightened to 60 lb-in. torque and a completely reversed external load of $\pm$200 lb has been applied, the average stress, using equation (2-41), was found from the example in Section 3.5 to be 21,818 psi. The average stresses calculated by using equations (2-47) and (2-72), were equal to 12,612 and 13,960 psi respectively, from examples 1 and 3 in Section 3.6. Now, assuming a sinusoidal load variation, the fluctuating stress at the mounting hole area can be plotted as a function of time from these analytical values, and is shown in Figure 34.

The fluctuating stress at the mounting hole area can also be plotted as a function of time from the experimental results of Sections 3.2 and 3.6 and are also shown in Figure 34.

Similarly, the stresses in the bolt were computed by using equations (2-3), (2-55) or (2-56) and (2-71), and the fluctuating stress in the bolt can be plotted. For example, when the bolt has been tightened to 20 lb-in. torque and a completely reversed external load $\pm$600 lb has been applied, the stresses in the bolt, in examples 3 and 4, Section 3.7, calculated

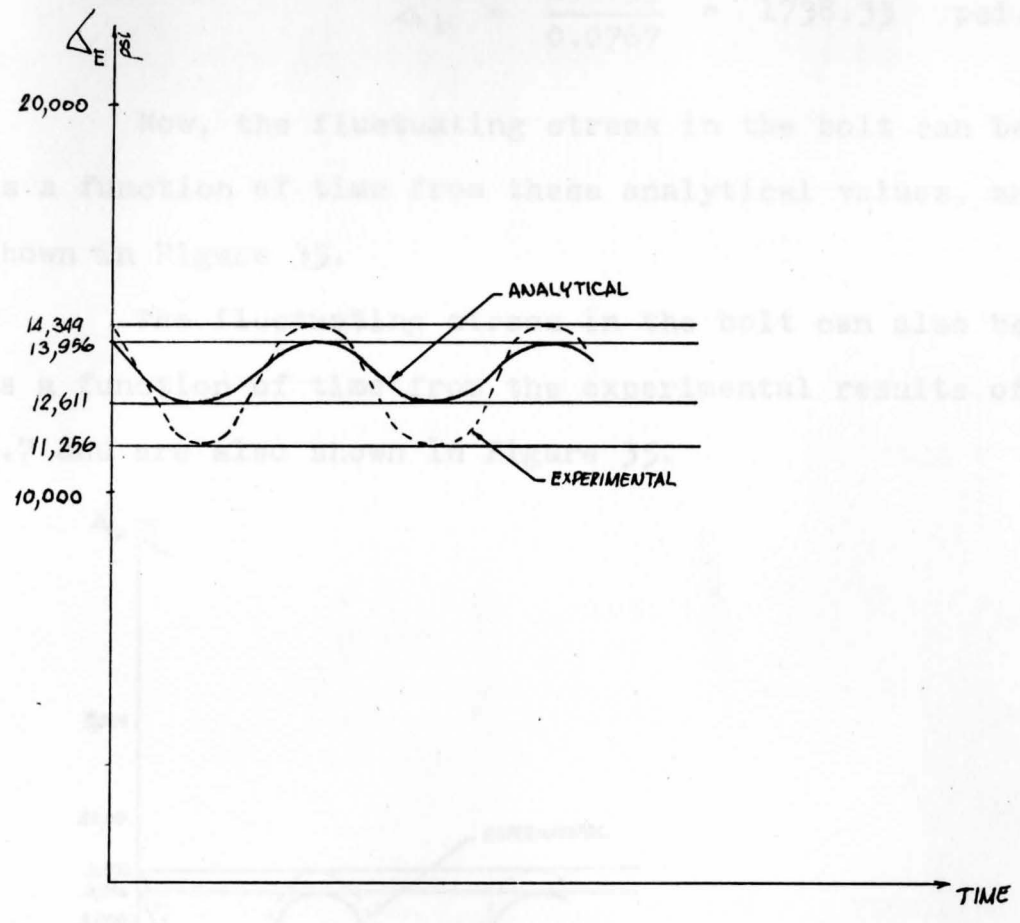

Figure 34 Fluctuating Stress in the Sign Face at the Mounting Hole Area

by using equations (2-55) and (2-71), were equal to 2229 psi and 3296 psi respectively.

The stress in the bolt calculated by using equation (2-3) follows:

substituting for T (20 lb-in.) in equation (3-3) gives

$$F_i = \frac{20}{.480\left(\frac{5}{16}\right)} = 133.33 \quad \text{lb.}$$

Substituting for F_i in equation (2-3) yields

$$\sigma_b = \frac{133.33}{0.0767} = 1738.33 \quad \text{psi.}$$

Now, the fluctuating stress in the bolt can be plotted as a function of time from these analytical values, and is shown in Figure 35.

The fluctuating stress in the bolt can also be plotted as a function of time from the experimental results of Section 3.7 and are also shown in Figure 35.

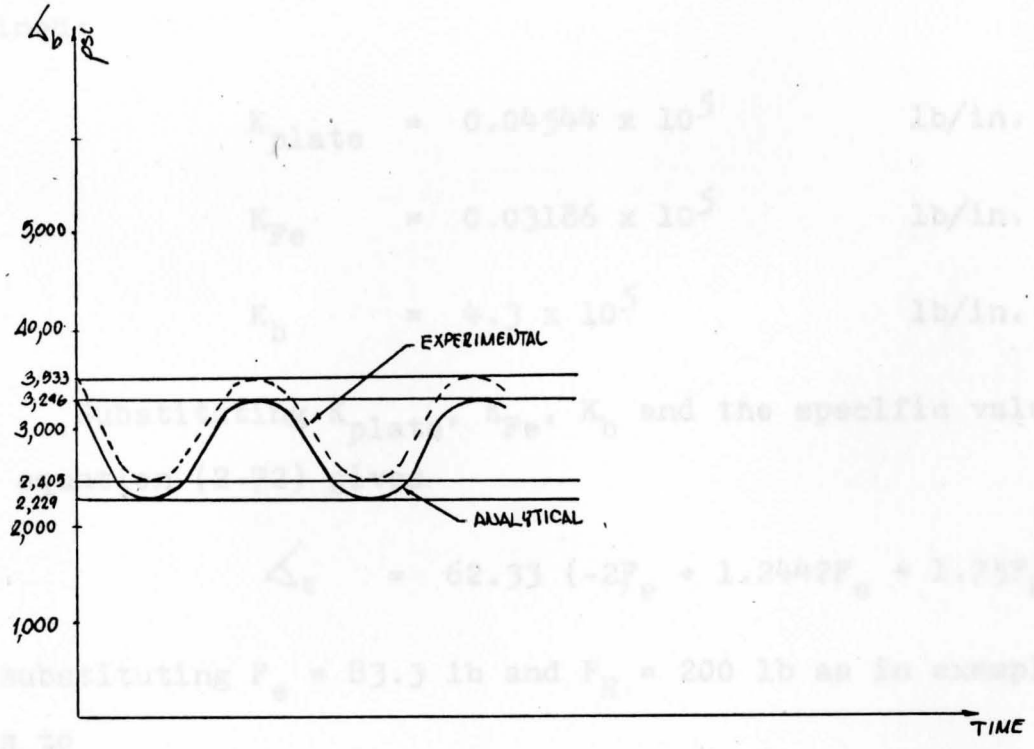

Figure 35 Fluctuating Stress in the Bolt

In a close examination of all the equations obtained in Chapter II, it was seen that the most sensitive parameter in those equations is x, which is the distance between the edges of post. In practice, it was very difficult to determine the exact value of x since the distance, x, may vary from 2" to $3\frac{1}{2}$" depending on the direction of loading. Therefore, the value

of x for each specific case was chosen from this range and the fairly accurate results obtained justify its use in each case. For example, in considering equation (2-72) used in the example 3, from Section 3.6, substitution of the typical values of x = 3", ℓ = 8", $\ell_b = 1\frac{3}{4}$", b = 10", t = 0.1", D = $\frac{5}{16}$", 2r = $\frac{3}{8}$", and $E_{sf} = E_b = 10 \times 10^6$ psi resulted in an average stress at point E of 13959.6 psi. If the value of x is changed to $3\frac{1}{2}$" and the others are unchanged, the following results are obtained:

$$K_{plate} = 0.04544 \times 10^5 \quad \text{lb/in.}$$

$$K_{Fe} = 0.03186 \times 10^5 \quad \text{lb/in.}$$

$$K_b = 4.3 \times 10^5 \quad \text{lb/in.}$$

Substituting K_{plate}, K_{Fe}, K_b and the specific values into equation (2-72) gives

$$\Delta_E = 62.33\ (-2F_e + 1.2442F_e + 1.75F_R),$$

and substituting F_e = 83.3 lb and F_R = 200 lb as in example 3, leads to

$$\Delta_E = 62.33\ (-62.98 + 350) \quad \text{psi}$$

$$= 17889.9 \quad \text{psi.}$$

It is thus seen from the above example that when the value of x is changed from 3 to 3.5", the value of average stress is changed, causing the difference between analytical and experimental results to change from 19 to 37 percent,

respectively.

The final consideration concerns the equations for R^a (2-24) and R^b (2-34). It was seen that the value of R^a from equation (2-24) must be less than F_R, and R^b from equation (2-34) must be greater than F_R. This then agrees with the conclusions from equation (2-17), that $|R^a| < |F_R|$, and from (2-30), that $|R^b| > |F_R|$. Thus, the assumptions included in this analyses were correct or can be said to hold true for this study.

APPENDIX A

Static Bending Stress Calculation

STATIC BENDING STRESS CALCULATION

The maximum bending stress at point A, due to load P, applied at point B, as shown in figure below can be expressed as follows:

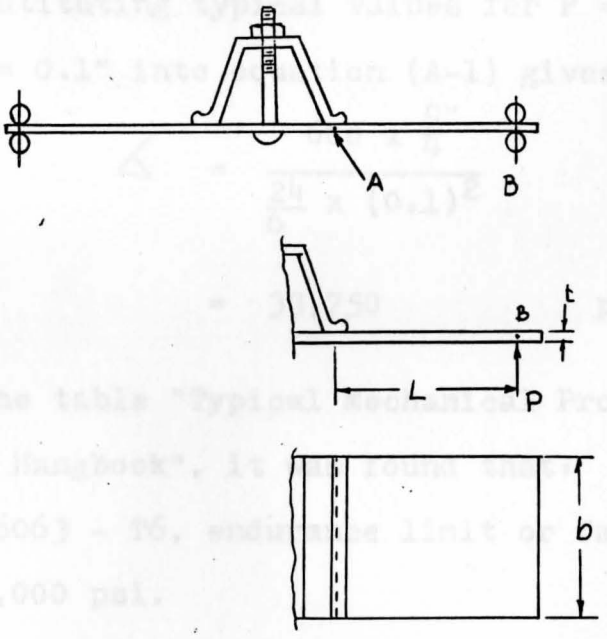

Assume: At point A, there is no bending moment from the initial preload F_i caused by tightening the bolt. Then from the simple bending stress equation,

$$\sigma = \frac{M}{S} \qquad , (A\text{-}1)$$

where: σ = bending stress, psi, and,

M = bending moment, lb-in.

I = moment of inertia, in^4

$$= \frac{bt^3}{12} \quad .$$

$$c = \frac{t}{2} \quad ,$$

$$S = \text{section modulus, in}^3$$

$$= \frac{I}{c} \quad ,$$

$$= \frac{bt^2}{6} \quad .$$

By substituting typical values for P = 600 lb, L = $\frac{9"}{4}$, b = 24" and t = 0.1" into equation (A-1) gives

$$\sigma = \frac{600 \times \frac{9"}{4}}{\frac{24}{6} \times (0.1)^2}$$

$$= 33{,}750 \quad \text{psi.}$$

From the table "Typical Mechanical Properties", page 26, "Alco Aluminum Hangbook", it was found that:

Alloy 6063 - T6, endurance limit or fatigue strength is equal to 10,000 psi.

Thus, it is seen that a 600 lb force at point B results in a bending stress at point A that exceeds the endurance limit stress by a factor greater than three.

REFERENCES

[1] Tarantine, F. J., "Testing of Signs and Their Support Against Wind Forces and Vibrations", Final Report. Report No. OHIO-DOT-15-75, Department of Mechanical Engineering, Youngstown State University, Youngstown, Ohio. August, 1975.

[2] Shigley, J.E., Mechanical Engineering Design. New York: McGraw - Hill Book Company, 1963.

[3] Faires, V. M., Design of Machine Elements. New York: Macmillan Company, 1963.

[4] Spotts, M. F., Design of Machine Elements. Englewood Cliffs, New Jersey: Prentice - Hall, 1961.

[5] Osman, M. O. M., et al. "On the Design of Bolted Connection With Gaskets Subjected to Fatigue Loading". Transactions of the ASME. Publication, Paper No. 76 - DET - 57.

[6] Roark, R. J., Formulas for Stress and Strain. New York: McGraw - Hill Book Company, 1965.

[7] Cernica, J. N., Strength of Materials. New York: Holt, Reinhart and Winston, INC., 1966.